AD NUMBER: AD0235571

LIMITATION CHANGES

TO:

Approved for public release; distribution is unlimited.

FROM:

Distribution authorized to US Government Agencies and their Contractors; Administrative/Operational Use; 31 Jan 1960. Other requests shall be referred to Air Force Cambridge Research Center, Bedford, MA 01731.

AUTHORITY

AFCRL ltr dtd 3 Nov 1971

AFCRC-TN-60-158

SCANNING TECHNIQUES

FOR

LARGE FLAT COMMUNICATION ANTENNA ARRAYS

J. P. Shelton
S. R. Perrino
A. B. Davis

Submitted by
Aero Geo Astro Corporation
1200 Duke Street (Box 1082)
Alexandria, Virginia

SCIENTIFIC REPORT NO. 1
Contract No. AF19(604)-5217

31 January 1960

Prepared for

ELECTRONICS RESEARCH DIRECTORATE
AIR FORCE CAMBRIDGE RESEARCH CENTER
AIR RESEARCH AND DEVELOPMENT COMMAND
UNITED STATES AIR FORCE
BEDFORD, MASSACHUSETTS

ABSTRACT

This report is a summary of the scientific progress on scanning techniques for large flat communication arrays during the first half of an eighteen-month study. The effort has been divided into experimental and theoretical projects. The experimental program has included phase shift techniques in open two-wire line and enclosed transmission line. The most promising results have been obtained with a circularly polarized coaxial configuration using the TE_{11} mode. Theoretical studies have been made in three areas -- circularly polarized phase shifters, multiple beams from linear arrays, and elimination of broadside resonance in traveling-wave arrays. It has been found that any circularly polarized component should be fed by a hybrid junction, the fourth output being terminated to absorb any reflected waves. Multiple-feed systems for arrays have been analyzed, and networks for connecting N inputs to N elements are presented, N being limited to 2^{13}m. A method for eliminating the broadside resonance in traveling-wave arrays in which the junction may be separated from the element is described. A tentative program for completion of the scanning system study is given.

TABLE OF CONTENTS

LIST OF ILLUSTRATIONS

List of Illustrations (Cont'd.)

I. INTRODUCTION

The work described in this report has been directed toward the improvement of scanning techniques for large flat communication antenna arrays. The statement of work indicates that emphasis is to be placed on investigation of techniques leading to low-cost of installation and maintenance with application to two-wire-line operation.

The sizes of the arrays that are involved over the frequency range 50 mc to 1000 mc vary from approximately 1000 feet to 50 feet square. Since the scan rate is slow and the power level is high, mechanically activated scan devices are considered. A low-cost installation would be typified by a two-wire-line configuration. An easily operated and maintained array, on the other hand, might not be an open-wire design, but rather a system of compact enclosed elements. Admittedly, open two-wire-line may offer the least resistive loss (except for ice or rain conditions) for feeding a 1000-foot array, so that its use is probably highly desirable for the lead lines.

In any event, consideration has been given to both open and enclosed transmission-line components. Experimental and theoretical results on various types of phase shifters are presented. The most promising new component is a coaxial circularly polarized unit that uses the TE_{11} mode.

The reasons for studying a circularly polarized phase shifter were a need for compact size and simple actuation, the requirement for simple relation between actuation and phase shift, and the possibility of cascading several units.

Theoretical study has been given to three topics -- circularly polarized phase shifters, multiple-beam arrays, and broadside resonance in traveling-wave arrays. Interesting and useful relationships have been developed in all three areas.

Multiple-beam arrays might seem inapplicable except for the frightening dimensions that phase shift mechanisms attain at the lower limits of the frequency range. Microwave switching, on the other hand, becomes simpler and more compact at lower frequencies; therefore, if multiple-beam arrays are feasible, scanning might better be achieved by switching among the inputs.

If a traveling-wave feed system is used, a resonance occurs when the relative phase is such that the reflections from all the coupling junctions add in phase. A method is presented for eliminating this resonance and also the resistive termination that characterizes traveling-wave arrays.

II. R-F PHASE SHIFTERS

2.1 Introduction

In considering the problems associated with the scanning of very large antenna arrays, the necessity of obtaining adequate phase shifting techniques

becomes mandatory. An approach to the problems encountered in the design of phase shifting components can be initiated by evaluating the four general characteristics imposed upon these units by normal system requirements:

1) Frequency independence
2) Minimum variation
3) Negligible loss
4) Continuous variation

Frequency independence is self explanatory in that the nominal bandwidth associated with any of these components should be at least compatible with the requirements for future system developments. The minimum variation of the phase shifting unit pertains to both the amplitude and phase error which may be prevalent in a single cycle of operation. Negligible loss must take into account not only the normal losses of VSWR, polarization and dissipation but the intangible properties which may be overlooked, such as coupling effects on mode purity or reflections which have to be absorbed. Continuous variation is concerned with the mechanical aspects of unit design. The two types of phase shifters which have been considered are the delay and the linear variation units. Both types have the intrinsic property of continuity, thereby eliminating some of the problems associated with complex motor drive sources.

Three types of transmission lines are applicable to the frequency range which must be considered. These consist of:

1) waveguide
2) coaxial
3) two-wire line or single-wire line (Goubauline)

Each of these transmission lines has, along with its obvious disadvantages, applicability to the problems associated with phase shifting techniques. The waveguide structure, although it becomes difficult to handle at frequencies much lower than 900 mc, is appealing from the abundance of information available to the design engineer. The mechanical difficulties encountered in maintaining electrical concentricity in coaxial lines can be overlooked due to the extremely useful bandwidth associated with the transmission line. Two-wire line or the single Goubau line is an inexpensive means of obtaining the desired results, but does impose a difficult barrier to the environmental designer.[1]

The following sections elaborate on the theoretical and experimental problems associated with these devices and conclude with the program status and proposed future effort.

2.2 Theoretical Considerations

A linear phase shifter may be defined through the means of excitation and the method of phase shift employed. In most of these units, excitation consists of the r-f network necessary to excite a circularly polarized mode in a transmission line. Circular polarization may be propagated in a number of ways depending upon the type of transmission utilized and the requirements

necessary to fullfill system applications. The tolerance problems encountered in this type of phase shifter will be analyzed with respect to polarization loss and probe mismatch.

2.2.1 Polarization Loss

A circularly polarized mode excited in a transmission line usually requires the output transmission to be sensitive to the polarization propagated in the structure. This is analogous to the problems associated with the transmission and reception of elliptically polarized waves. An expression has been derived by Sichak and Milazzo which relates the absolute magnitudes of an induced voltage in an elliptically polarized receiving source to an elliptically propagated wave;[2]

$$V = K\left[1 \pm \left(\frac{2r_2}{r_2^2+1}\right)\left(\frac{2r_1}{r_1^2+1}\right) + \left(\frac{r_2^2-1}{r_2^2+1}\right)\left(\frac{r_1^2-1}{r_1^2+1}\right)\cos 2\alpha\right] \qquad (2\text{-}1)$$

where

- K = Constant
- r_1 = Axial ratio of an elliptically polarized wave associated with the recurving source.
- r_2 = Axial ratio of the propagated wave.
- α = The angle between the direction of maximum amplitude associated with the two waves under consideration.

The $\pm$ sign is + if both r_1 and r_2 are of the same sense and - if they are opposite. In the case where both are of the same sense, the maximum variation due to rotation of one source relative to the other is of interest; application of $\cos 2\alpha = \pm 1$ to Eq. (2-1) yields

$$\frac{V^2 \text{ max.}}{V^2 \text{ min.}} = \frac{(r_2 + r_1)^2}{(r_2 r_1 + 1)^2} \quad \text{or} \quad \frac{(2r)^2}{(r^2+1)^2} \qquad (2\text{-}2)$$

The quantity shown in Eq. (2-2) is sometimes referred to as the WOW of a system. This value does not take into account the polarization loss of the system, but only the variation due to the presence of an elliptically polarized wave. Of course, this problem is resolved if either source is truly circular. Figure 1 is a curve of the interesting portion of this equation, and relates the dependence of the axial ratio associated with the input and output ports of a phase shifter with the maximum allowable WOW of a system. The importance of this relationship can be best illustrated by considering what effect a 1db variation in the output amplitude of a phase shifter might have on an antenna having a very low side lobe level requirement. The 1db variation would in effect leave no control over the side lobe level of the antenna.

The results indicated in Eq. (2-2) will only give the loss due to the WOW of the system. When r_1 becomes circular, the maximum WOW is described by the

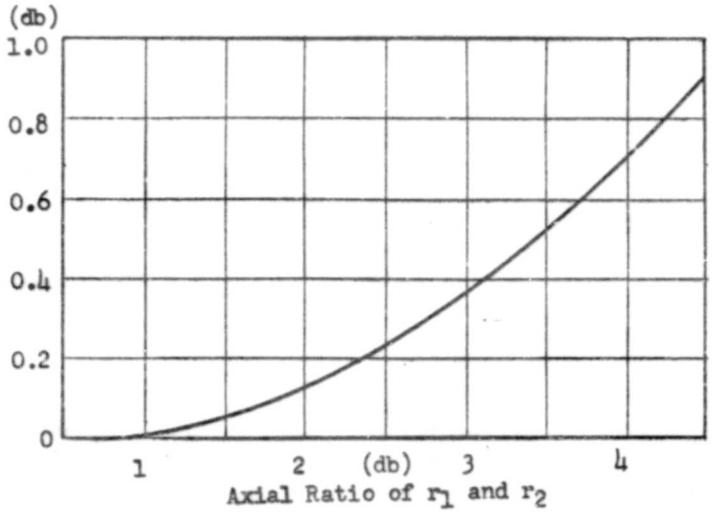

Figure 1. WCW vs. Axial Ratio of Exciting Elements in a Phase Shifter.

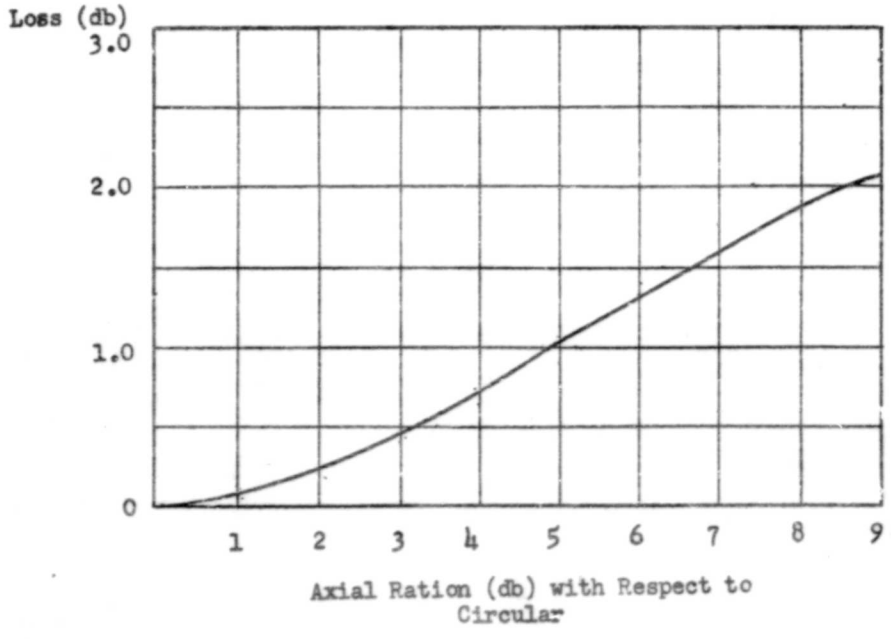

Figure 2. Maximum Loss Due to Variation in the Polarization or Axial Ratio of Two Waves.

polarization of r_2. In the case where the sources are of opposite sense, the maximum variation is described by

$$\frac{V^2 \text{ max.}}{V^2 \text{ min.}} \qquad \frac{(r_2 - r_1)^2}{(r_2 r_1 - 1)^2} \tag{2-3}$$

In this case, where r_1 is less than r_2, Eq. (2-3) yields a solution which might conceivably be utilized in practical applications. This is readily resolved by now considering the polarization loss due to the interaction of an elliptically polarized wave imposed in an elliptically polarized receiving source. The maximum loss which will result from variation in the axial ratio of the two sources of a phase shifter can be computed by observing the relationship of

$$\frac{V_2 \text{ max.}}{V_1 \text{ max.}}$$

where V_2 maximum would be the resultant of a change in the axial ratio of one source of the phase shifter.

The maximum loss will occur in a system of like sensed ports when one port is circular and the other port is linear. The maximum loss is then 3 db. The maximum loss in a system of unlike sources will be obtained when both ports are circular; one being right hand and the other being left hand, the maximum loss then being infinite.

For the practical case when both sources are of the same sense,

$$P \text{ max.} = \frac{2(r_o^2 + 1)}{(r_o + 1)^2}$$

where

r_o = the new value of r_1 or r2.

The curve shown in Figure 2 illustrates the polarization loss incurred due to departures from the hypothetical system of two circularly polarized ports of a phase shifter. It is now quite evident that in the case of the two oppositely sensed sources, the polarization loss of the system must exceed 3 db.

2.2.2 Effect of Probe Mismatch

If the phase shifter incorporates a power divider, phase shifter in one of the outputs to provide phase quadrature, and orthogonal probe transitions to the cylindrical transmission line, the effect of the probe mismatch is of interest. If a conventional two-way power divider is used, the effects appear in degradation of input impedance and ellipticity of polarization set up in the cylindrical guide.

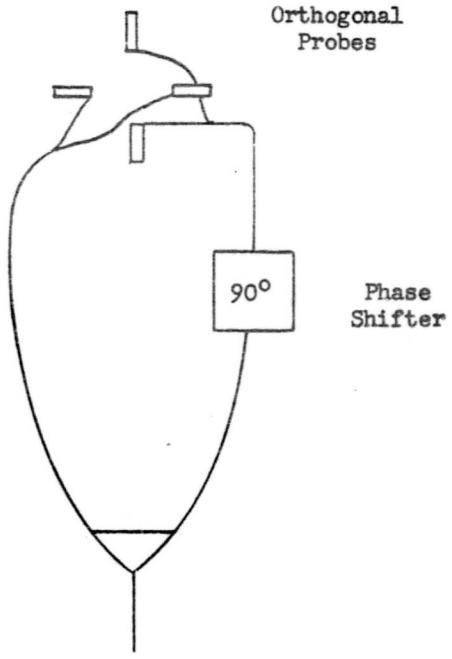

Feed Network for Circular Polarization

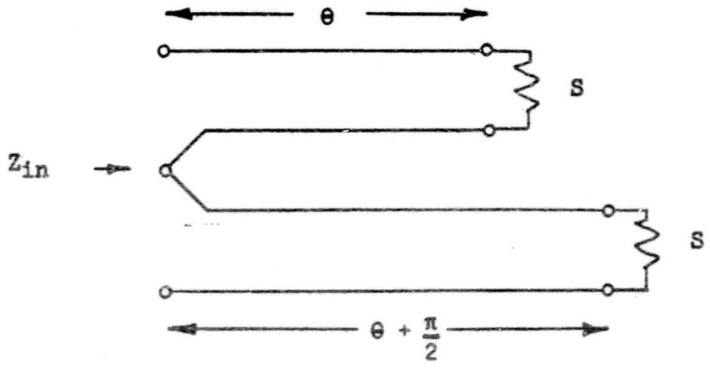

Equivalent Circuit

FIGURE 3. DIAGRAMS OF LOSSLESS CIRCULAR POLARIZER

With reference to the network shown in Figure 3, it is seen that the normalized input impedance is given by

$$Z_{in} = 1/2 \left[\frac{S + j \tan\theta}{1 + j S \tan\theta} + \frac{1 + j S \tan\theta}{S + j \tan\theta} \right]$$

$$= 1/2 \frac{(1 + S^2)(1 - \tan^2\theta) + 4 j S \tan\theta}{S(1 - \tan^2\theta) + j \tan\theta (1+S^2)}$$

The reflection coefficient is written

$$\rho_{in} = \frac{Z_{in}-1}{Z_{in}+1}$$

$$= \frac{(1 + S^2)(1 - \tan^2\theta) + 4 j S \tan\theta - 2 S (1 - \tan^2\theta) - 2 j \tan\theta (1 + S^2)}{(1 + S^2)(1 - \tan^2\theta) + 4 j S \tan\theta + 2 S (1 - \tan^2\theta) + 2 j \tan\theta (1 + S^2)}$$

$$= \frac{(1 - S^2)^2 (1 - j \tan\theta)^2}{(1 + S^2)^2 (1 + j \tan\theta)^2}$$

$$\rho_{in} = \frac{(1 - S^2)^2}{(1 + S^2)^2}$$

The input standing-wave ratio in terms of the probe standing-wave ratio is

$$S_{in} = \frac{1 + |\rho|}{1 - |\rho|} = \frac{1 + S^2}{2 S}$$

It can easily be seen that the input VSWR is considerably better than that of the individual probes, as for example, a probe match of 2:1 is reduced to 1.25:1.

This desirable impedance characteristic is obtained at the expense of loss of circularity in the transmitted mode. The analysis of this effect is best carried out by following the waves through the network, as shown in Figure 4. The incident wave passes through the power divider and the two components are reflected from the probes. The transmitted wave sets up a circularly polarized mode; the reflected wave arrives back at the power divider with one component retarded by 180 degrees. This plus-minus mode will not pass through the power divider and is reflected back toward the probes. This energy, after being transmitted by the probes, sets up a circularly polarized mode of the opposite sense. The second reflected wave arrives back at the junction with both components in phase and returns to the input, setting up the VSWR previously found by impedance analysis. As is shown in the figure, the results in terms of probe reflection coefficient are

Axial ratio: Voltage AR $= \frac{1 + |\rho|}{1 - |\rho|} = S$

Reflection coefficient $|\rho_{in}| = |\rho|^2$

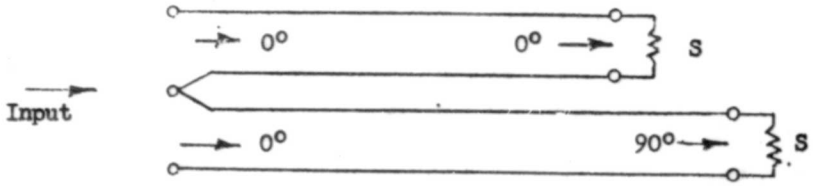

Incident Wave

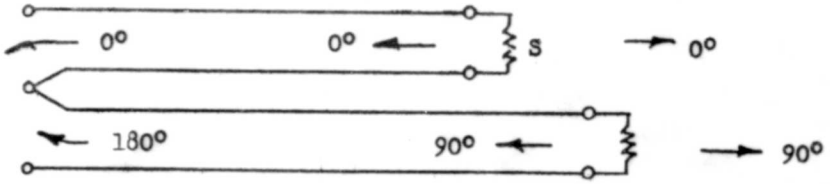

First Transmitted and Reflected Waves

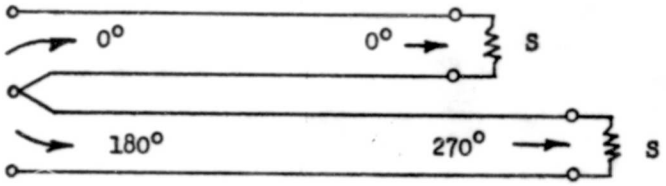

Second Incident Wave

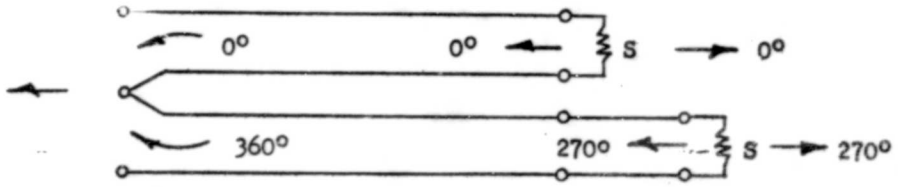

Second Transmitted and Reflected Waves

FIGURE 4. WAVES SET UP BY MISMATCHED PROBES

It is interesting to note that both the reflected wave and the transmitted oppositely sensed wave are eliminated if the power divider and phase shifter are replaced by a hybrid junction. The fourth part of the hybrid junction can be terminated to absorb the wave reflected from the probe. The relatively severe variation in phase shift, insertion loss, and VSWR is eliminated in favor of uniform phase shift, matched impedance, and small but uniform insertion loss.

2.2.3 Design Approach

The general parameters of phase shift design, in respect to the theoretical considerations evaluated in the preceding two sections, can now be stated.

a) Bandwidth > 50 percent
b) VSWR $\leq$ 1.17:1
c) WOW $\leq$ 0.3 db
d) Loss < 0.8 db
e) Phase shift deviation $\leq \pm 5$ degrees

Since bandwidth enjoys a predominant role in the design of phase shifting structures, careful consideration must be taken in the employment of transmission line techniques. Many techniques have been evaluated only from electrical requirements, but there are many mechanical aspects which must be given equal consideration. Figure 5 illustrates a few methods capable of meeting the above parameters. Most of the methods shown here are mechanical variations of the Fox phase shifter[3]. The basic electrical properties of this phase shifter consist of exciting the linear TE_{11} mode in circular waveguide and then transforming this, through a fixed 90-degree delay orientated at 45 degrees to the excited wave, into a circularly polarized wave. The same technique is used in the transition end of this unit. Phase shift is then obtained by rotating one end in respect to the other.

A modification to this technique, which has a multitude of mechanical advantages, would be the excitation of the TE_{11} linear mode in coaxial transmission line. Orthogonal to this initial mode would be a second TE_{11} coax mode with a 90-degree phase difference between the two. This is illustrated in Figure 5c. The mechanical advantages of this system, as illustrated in Figure 6, are the weight and size reduction due to the utilization of coax, the advantage of placing the entire motor-drive system within the phase shifter and the advantage of rotating only the inner section of the coax. It should be noted that the rotary joint may be eliminated by placing a rotating center section having a 180-degree differential phase shift in the unit. This is illustrated in Figure 7.

The bandwidth capabilities of the coax-phase shifter are not impaired by the fixed phase shift required to excite circular polarization in the line. Present work in the field of fixed phase shift units has produced r-f networks capable of maintaining the proper characteristics over a 4:1 frequency band[4].

A. Pin Phase Change

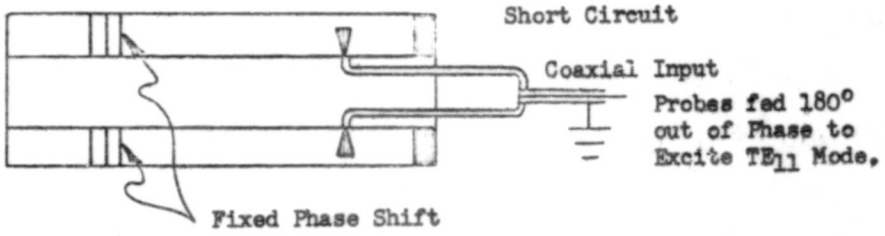

B. Two-Wire Line Operating in Balanced Mode.

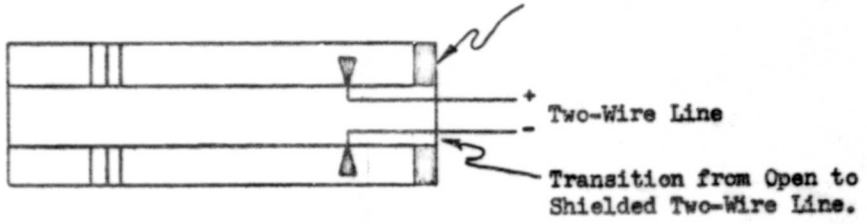

C. Two-Wire Line

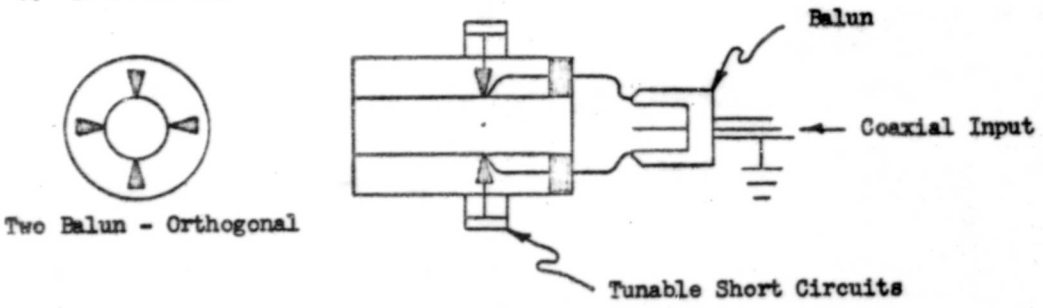

FIGURE 5. VARIOUS METHODS FOR EXCITING THE CIRCULARLY POLARIZED MODE IN COAX

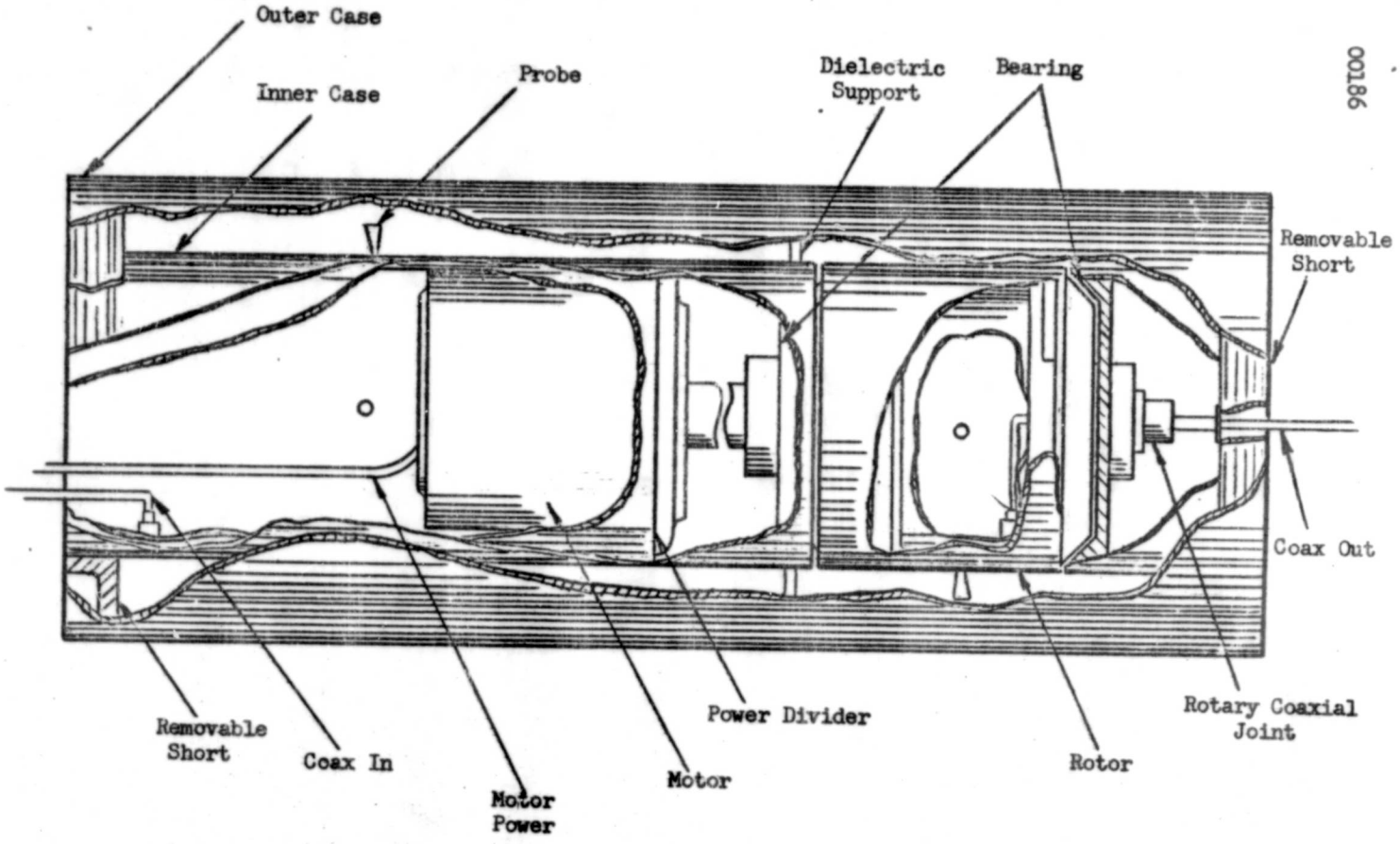

FIGURE 6. PROPOSED DRIVE SYSTEM FOR COAX LINE PHASE SHIFTER

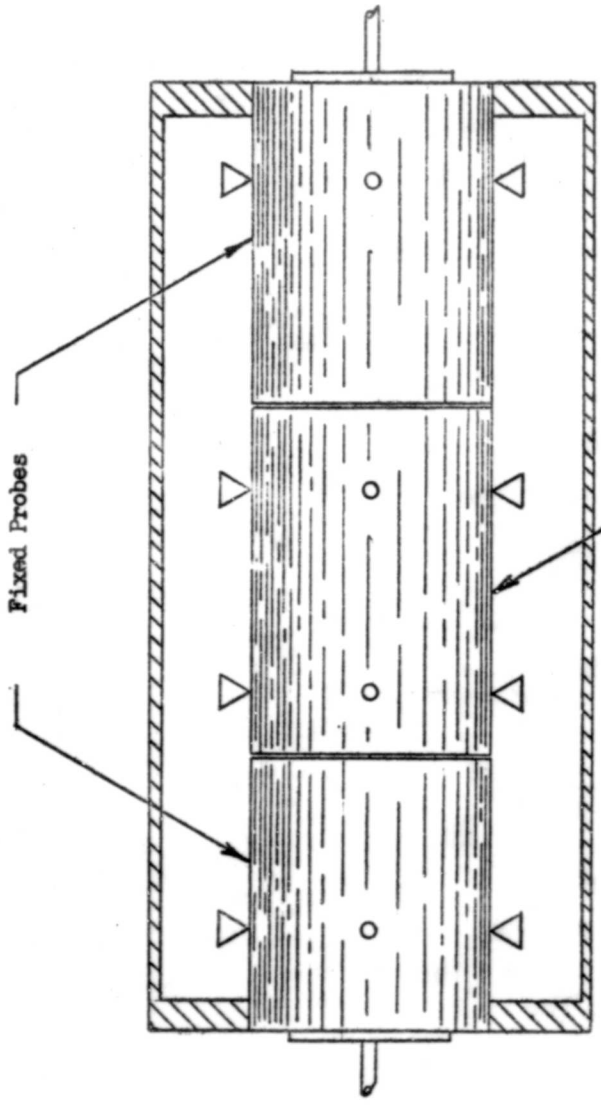

FIGURE 7. MODIFIED FOX PHASE SHIFTER

Information which may further be extracted from Eq. (2-1) is the maximum variation in axial ratio which may be accepted while still maintaining the system requirement of 0.3 db WOW. If the axial ratio of one source approaches circular then the other part varies by the relationship

$$r_1 = \frac{b - r_2}{1 - b\, r_2}$$

where

$$b = \text{WOW (0.3 db)}$$

The curve shown in Figure 8 illustrates the maximum variation in axial ratio that may be tolerated. The limiting function on this expression is imposed once again when loss is considered. Consequently the interdependence of WOW, polarization loss, and VSWR can determine the complete experimental program to be carried out on a project of this type.

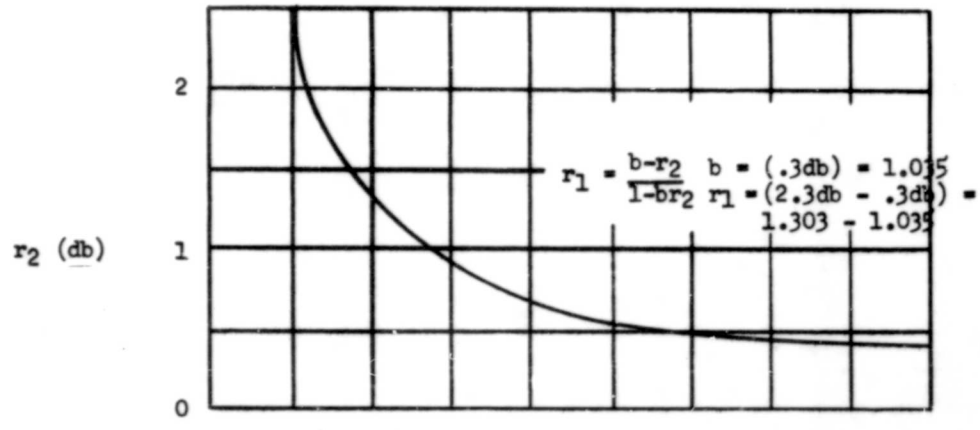

Figure 8. Variations of r_1 as r_2 Changes from Maximum to Minimum Ellipticity (2.3 db 0.3 db).

2.3 Two-Wire Line Considerations

The general properties of two-wire transmission line with respect to array design have been investigated by many authors[5,6,7]. The techniques referenced have formed the basis of further study in the scanning of two-wire line arrays and need not be further explained.

The normal balanced mode in two-wire transmission line, shown in Figure 9, lends itself to a simple analysis of the field variation due to discontinuities placed within the structure. The characteristic impedance of two-wire line is related to the capacitance per unit length which is related to the difference of potential such that[8],

$$Z_o = \frac{1}{vC} = 120 \cosh^{-1} \frac{D}{d}$$

Consequently the potential equations are obviously related to Z_o and the field distribution will be dependent upon any obstruction between the lines. Using these relationships to our advantage can result in a feasible approach to scanning techniques. Due to the effects on field distribution of an obstruction between the lines, the obstacles must be placed between radiating elements. Different phase shifting devices are shown in Figures 10a, b, and c.

The pin dielectric referred to in Figures 10a, b, and c is a modification of the work accomplished by Bowie and Chadwick[9]. Formulae (for the value of the effective dielectric constant, k, of an artificial dielectric) can be derived for "metallic delay media" by an equivalent transmission line method of

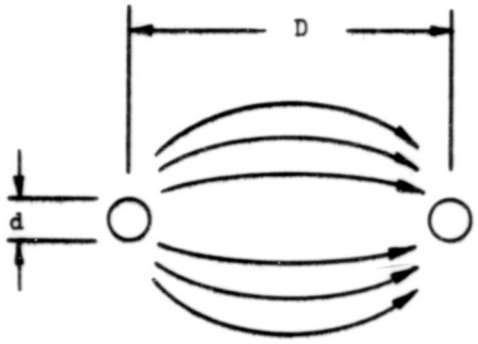

Figure 9. Field Configuration - Two-Wire Line in Balanced Mode.

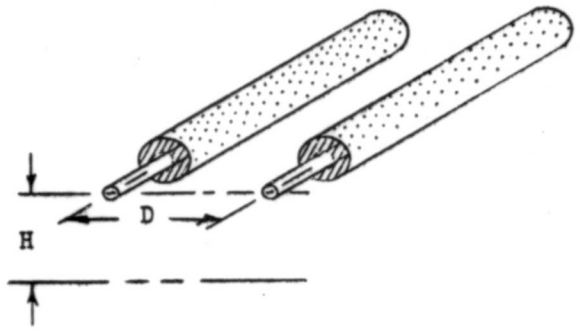

(b)

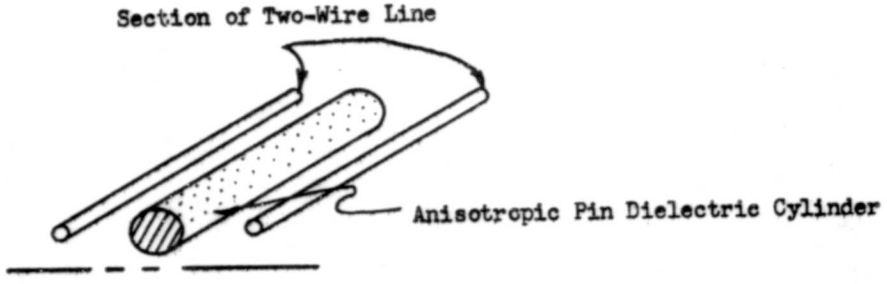

(a)

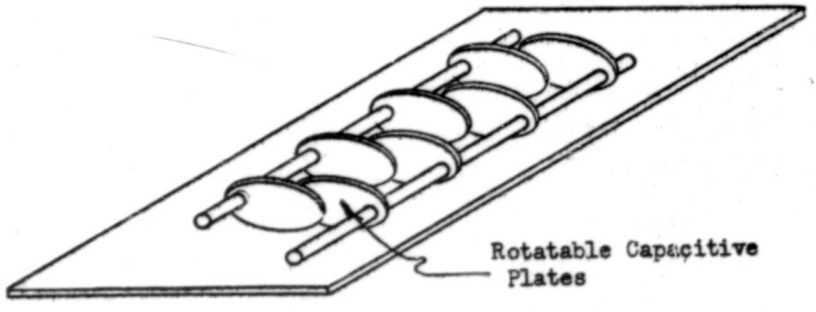

(c)

Figure 10. Phase Shifting Techniques in Two-Wire Line.

analysis which was originally proposed by Kock[10].

$$K' = \left(\frac{\lambda}{\lambda'_g}\right)^2 + \left(\frac{\lambda}{\lambda_c}\right)^2$$

where

λ = Free-space wavelength.
λ'_g = Wavelength in the material.
λ_c = Cut-off wavelength.

The value of the effective dielectric constant, K', due to a uniform array of obstacles embedded in base material is given by the expression

$$K' = N^2 = K \text{ base } (1 + N\alpha 10/E_o)$$

where

10 = "Equivalent polarizability" of a single obstacle in free space.
N = Number of obstacles per unit volume.
E_o = Intrinsic permitivity of free space.

A cylindrical pin dielectric phase shifter has been made for operation in the 900 mc frequency range. The base dielectric material is a mixture of teflon and epoxy resins having a dielectric constant of about 1.1. Experimental results of the pin dielectric are reported in Section 2.4.

2.4 Experimental Results

2.4.1 Introduction

The data included in this section were taken to provide experimental verification of the theoretical study of several types of continuously variable 360 degree phase shifters for radio frequency applications.

At present, three types of phase shifters are undergoing experimental investigation. These are a coaxial phase shifter, spiral phase shifter, and a dielectrically loaded two-wire line. The experimental results achieved with each will be presented in this order.

2.4.2 Coaxial Phase Shifter

The first step in developing a coaxial phase shifter was to construct a test unit in which the TE_{11} mode could be excited. The frequency range chosen for experimental testing was 900 mc to 1400 mc. The test unit consists of two sections of brass tubing 25 inches long. One has an I.D. of 5.76 inches and the other an O.D. of 3.5 inches. These two tubes were assembled coaxially and held in place by brass spacer disks which also served as tunable short

circuits. A photo of the disassembled unit is shown in Figure 11. The cut-off frequency for the TE_{11} mode in this assembly is approximately 866 mc. The initial choice of probe configuration to excite the TE_{11} mode in coax was a brass rod .090 inch in diameter and 0.5 inch long. For initial measurements only two probes were used. The probes were placed on the outer surface of the inner conductor and spaced diametrically opposite one another. They were fed electrically 180 degrees out of phase by making one feed cable longer by one-half wavelength at 1000 mc. The cable used was RG58-U, which has a velocity of propagation of 65.9 percent of free space. This configuration was designed to excite a linearly polarized TE_{11} mode.

Figure 12 shows a plot of the VSWR of a probe mounted in free space and loaded with various sizes of disks. One probe one inch long and loaded with a one inch diameter disk was then tried. It was found that the VSWR of this probe could be matched to 1.3:1 by proper adjustment of the brass short circuit behind it. Since this shape showed promise, the next step was to mount two identical probes in the unit with a one-inch capacitive disk on each. The two probe unit with its associated feed cables was fed through a T.N.C. type tee connector and a Hewlett-Packard slab line. The following measurements were taken on this unit:

1) Isolation between probes - 1.4 db.
2) VSWR, both elements, fed 180° out of phase - 30:1.
3) VSWR, one element only, the other element terminated in a 50-ohm coax termination - 1.36:1.
4) VSWR, one element only, the other element terminated in an open circuit - 18:1.
5) VSWR, one element only, the other element terminated in a short circuit - 9.0:1.

The above measurements, made at 1000 mc, indicated that the probes, loaded with the capacitive disks, would radiate but were too tightly coupled. An isolation or coupling figure of 1.4 db indicates that approximately 72 per cent of the energy radiated at either probe is coupled directly to the other probe. This coupled energy is reflected back down the line towards the generator causing the high input VSWR. By computation, these values of incident and reflected energy yield a theoretical VSWR very close to the measured value of 30:1. This provides a check on the validity of the measurement technique.

Several new probe designs were tried, and the best results were achieved with a cone shaped probe 0.85 inches long, 5/16 inches in diameter at the large end and .090 inches at the small end. A matching structure was also built to minimize the mismatch caused by feeding the two lengths of parallel 50 ohm line with the coaxial "T" type connector. A quarter-wave transformer section of 70 ohm coax (RG140/U, V.P. = 69.5 percent) was built. This is

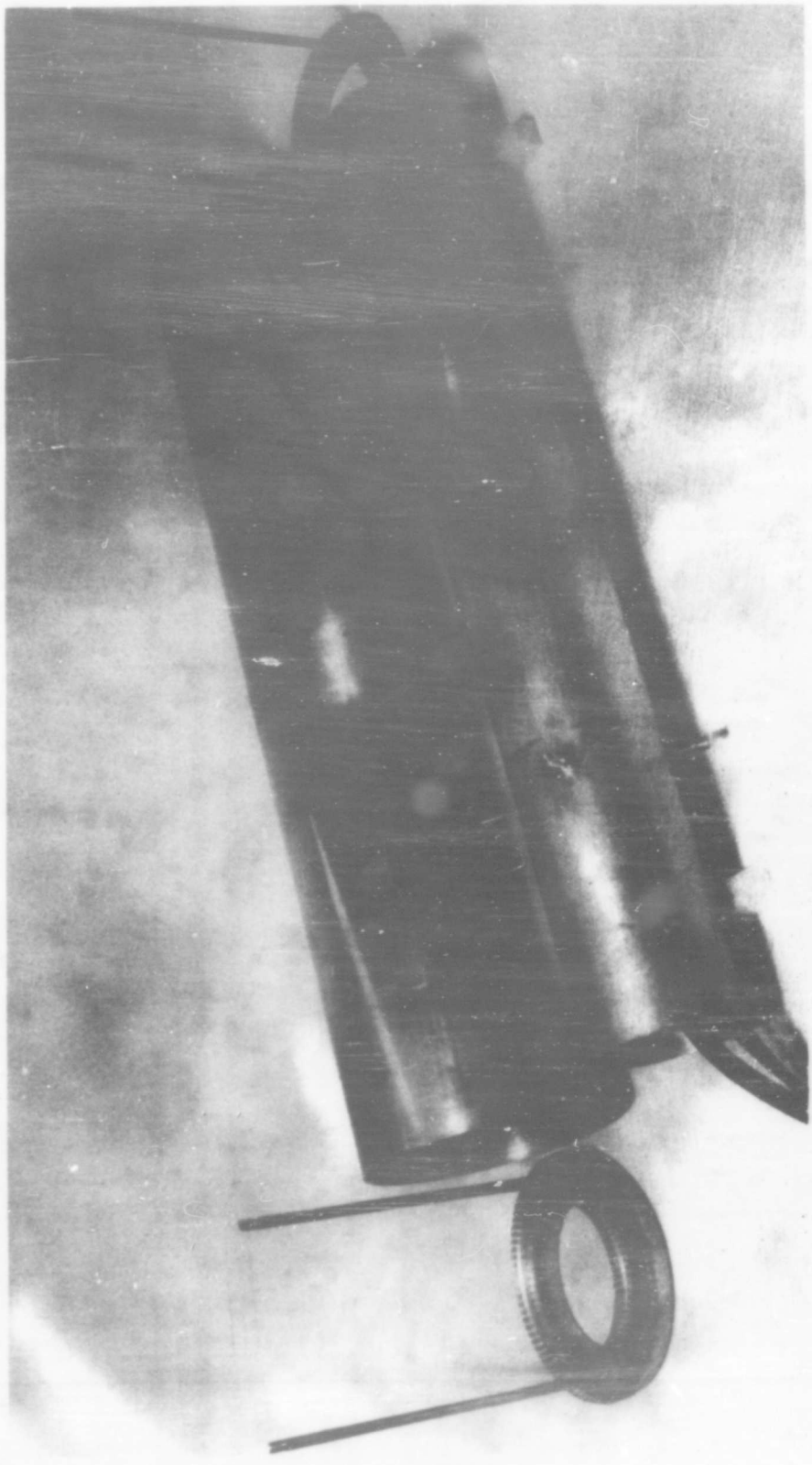

Figure 11. Coaxial Phase Shifter.

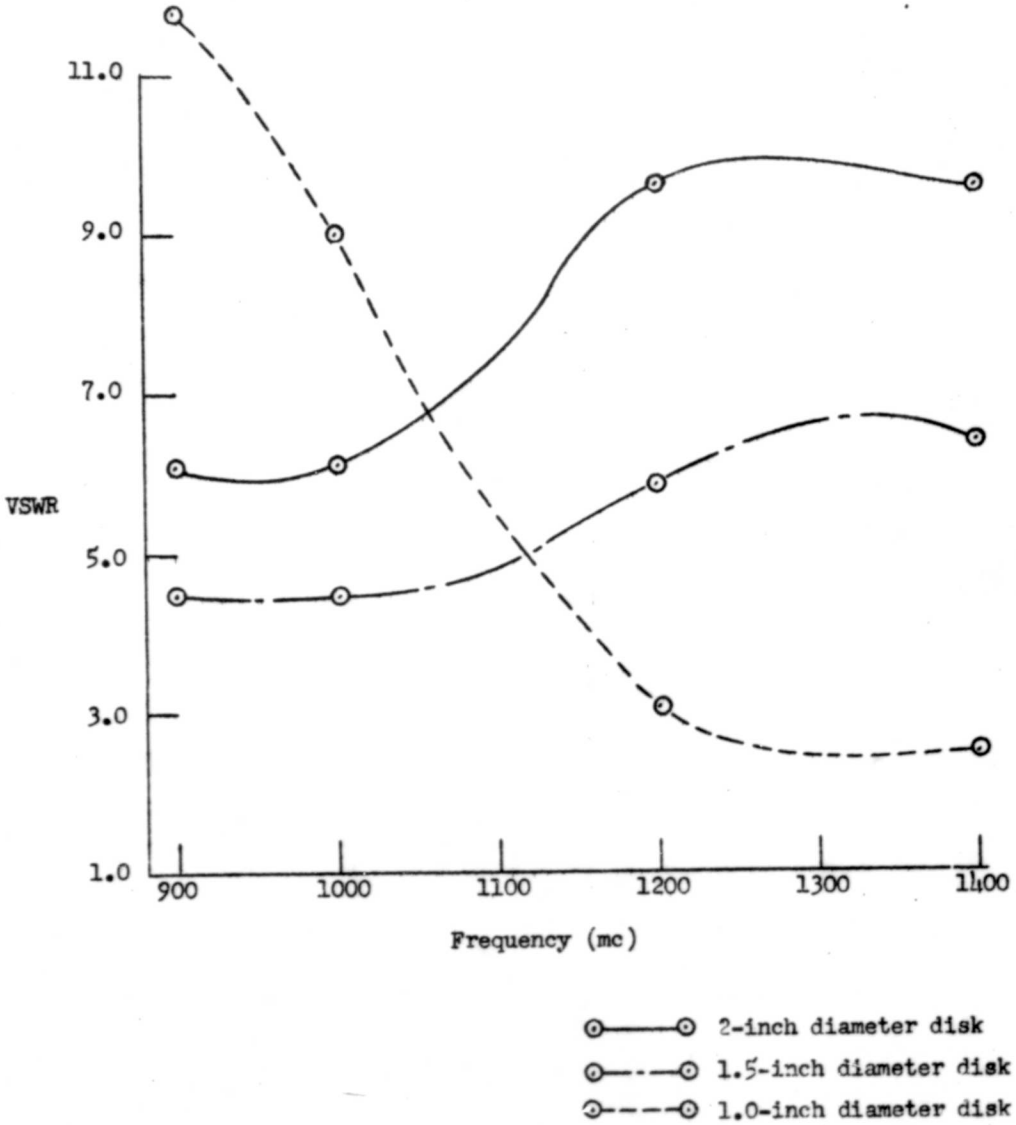

Figure 12. VSWR of Probe End-Loaded with Various Sized Disks

shown schematically in Figure 13. The input VSWR of the TNC tee and transformer section was 1.63:1 with the output arms loaded with 50 ohm coax terminations. The maximum VSWR of the coax terminations was 1.12:1 at this frequency. The VSWR's of the probes were measured separately and found to be 5.0:1 with the other probe loaded and 3.5:1 with the other probe terminated in an open circuit. A check of isolation showed 7.2 db isolation between elements. Although the input VSWR of the probes and feed harness was not as low as was assumed possible, measurements were made to determine the relative field strength at positions of angular displacement around the coax. Figure 14 shows a plot of this relative field strength. The results of these experiments indicated that the proper mode was being excited.

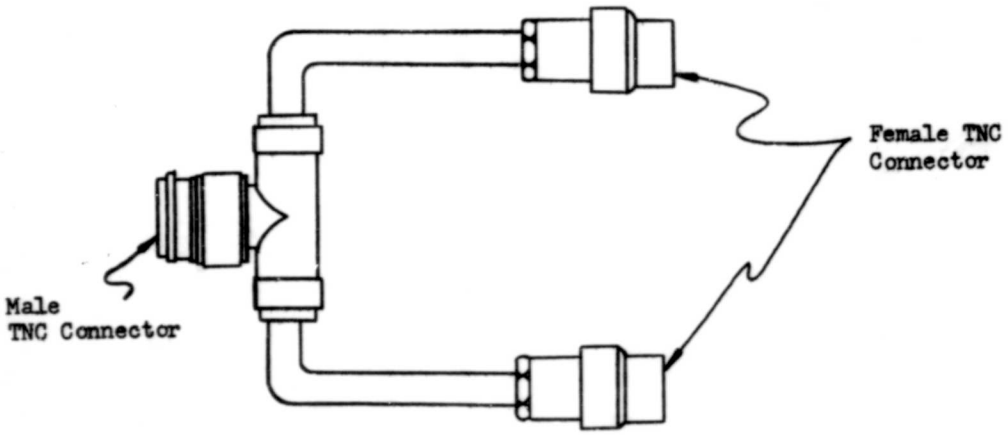

$L = \frac{3\lambda}{4}$ at 1000 mc

Z_o = 70 ohm

Figure 13. Quarter-Wave Transformer - 70 ohm Coax.

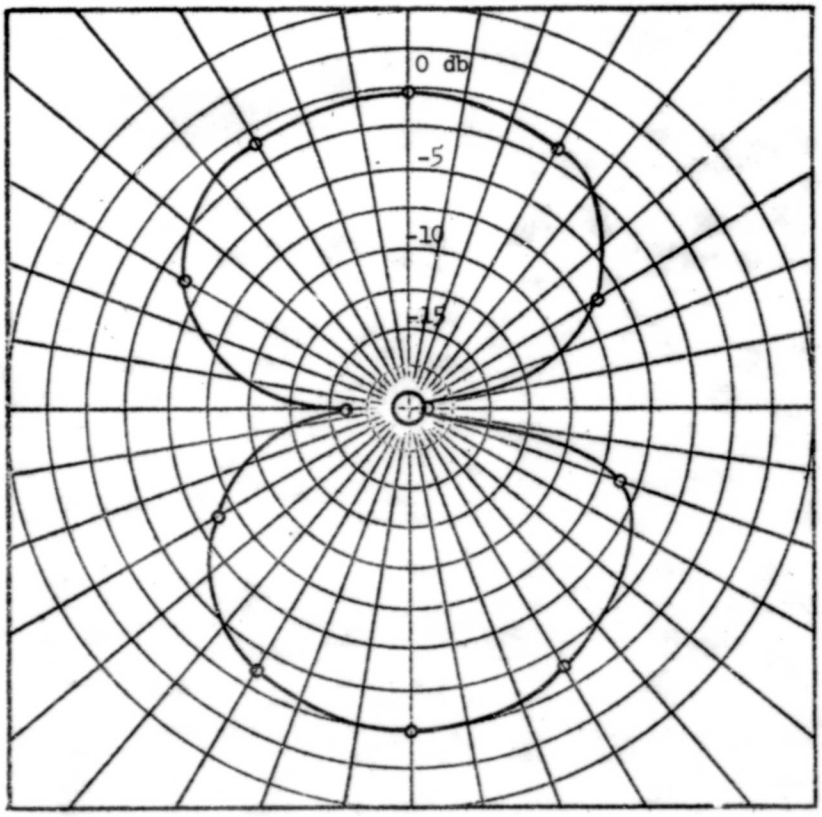

Figure 14. Relative Field Strength of Two Probe Unit.

In attempting to improve the match of the feed harness it was found that after allowing for the length of center conductor of the connectors, a transformer section of 70 ohm coax was too short to allow the attachment of connectors. To solve the feed problem, a three-quarter wavelength feed harness was designed using 70 ohm coax (RG140/U). Although this made the test unit more narrow band, it was felt that the bandwidth would be sufficient for the purpose of the experiment. The input VSWR of the feed harness was then measured with both outputs loaded. A plot of these measurements is found in Figure 15. Next, the two conical probes were mounted in the coax and the shorting plate adjusted for minimum reflection from the probes at 1000 mc. The shorting plate serving as the spacer at the opposite end of the test piece was slotted to permit the attachment of four tapered pieces of resistance card. This served as a load for the radiating elements. The probes were fed out of phase through the feed harness by cutting feed cables to length. A plot of the VSWR is found in Figure 16. It will be noted that the unit is narrowbanded and that the minimum value of VSWR falls at the design frequency. Measurements of the relative field strength were then made to determine the field configuration within the coax. A plot of these data is found in Figure 17. The plot of relative field strength indicated excitation of the desired mode, the axial ratio being of the order of 7 db.

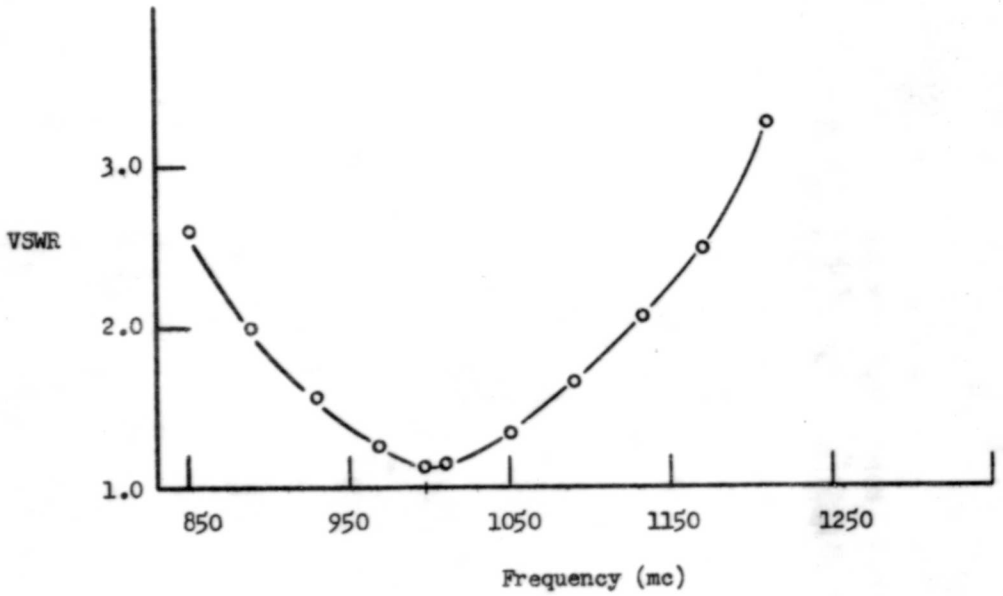

Figure 15. VSWR of Coax Feed Harness.

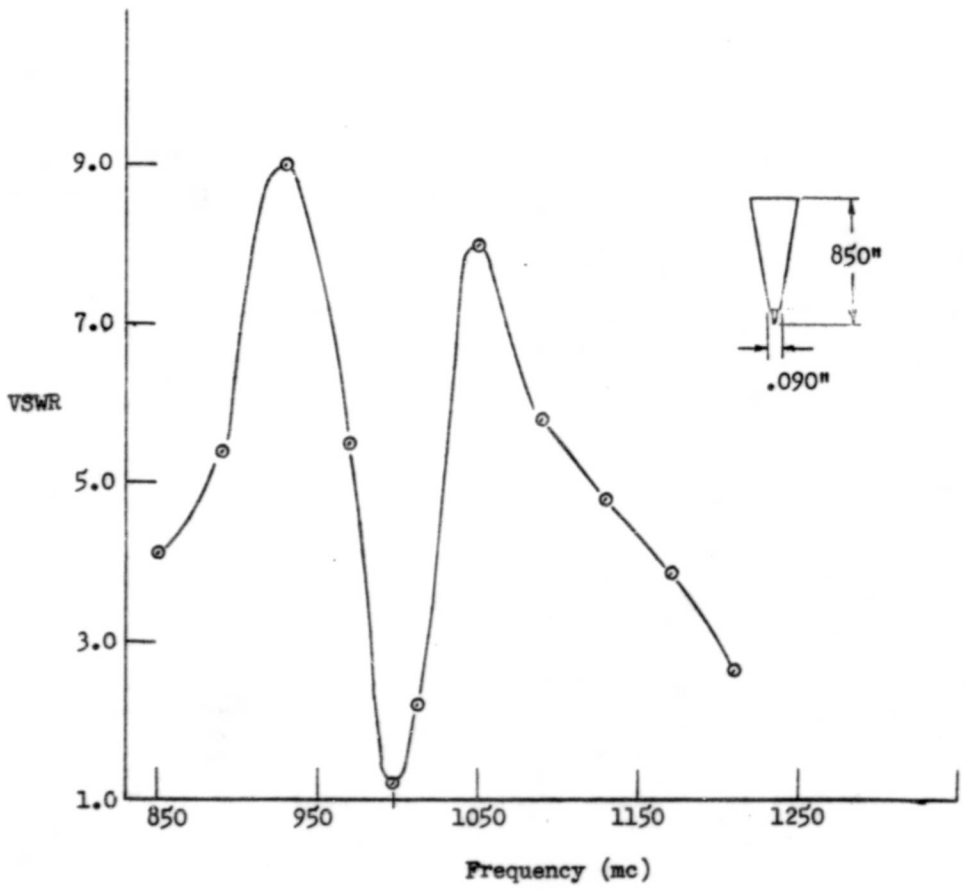

FIGURE 16. VSWR OF TWO PROBE UNIT

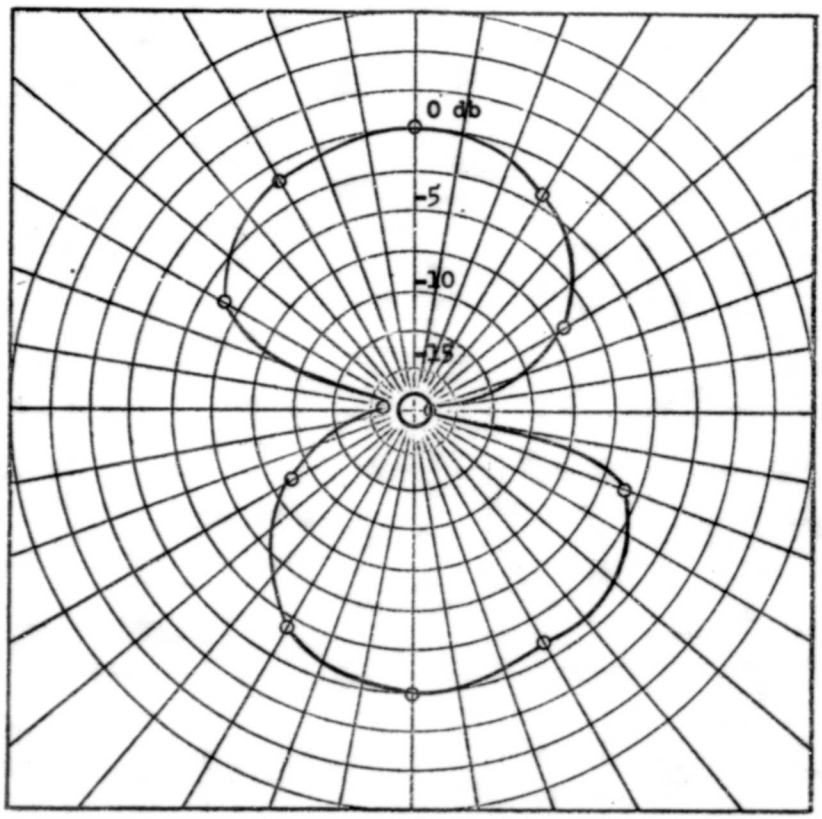

FIGURE 17. RELATIVE FIELD STRENGTH - TWO PROBE UNIT

Two more probes were added in the coax, spaced 90 degrees from the existing probes and diametrically opposite one another. The addition of the two probes dictated the need for a change in the feed harness. Each probe is fed by a cable which is shorter than the adjacent cable by 90 degrees. A three-quarter wavelength matching structure feeds these four cables by using a coaxial tee on each arm of the matching structure. The cable used in this harness has a characteristic impedance of 50 ohms. The input VSWR of the four probe unit was measured and found to be 1.36:1. Relative field strength measurements were then made of two probes 180 degrees apart and fed 180 degrees out of phase, the other two outputs being loaded with 50 ohm terminations. This test was repeated with the other set of probes. These plots of relative field strength indicated that the two inactive probes did not affect the field created by the two driven elements. A check of isolation showed that two probes 180 degrees apart were isolated by 9 db while one of the passive probes was isolated from the active pair by greater than 30 db. This was as expected because of the symmetry of the probes and field.

All four probes were then fed simultaneously, each 90 degrees out of phase electrically with the adjacent probe. A plot of relative field strength, Figure 18, yielded an axial ratio of 8 db. Upon inspection of the feed harness it was found that each arm of the harness fed two probes that were 90 degrees out of phase electrically and 90 degrees apart physically. In all previous measurements one arm of the feed harness had fed two probes which were 180 degrees out of phase electrically and physically. The feed arrangement was changed accordingly and a new plot of field strength was made. This is found in Figure 19. It will be observed that the axial ratio improved to 2.8 db. This deviation from circularity is caused by the mismatch of the individual probes. Impedance measurements were made of the existing probe and it was found that to properly match a two probe unit, capacitive reactance should be added. The large diameter of the probe was increased from .275" to .350" and the impedance of the two probe unit measured. The resulting impedance plot shows the VSWR improved to a value of 1.1:1.

In summary, satisfactory progress has been made on the development of a TE_{11} mode coaxial-line circularly polarized phase shifter. Further effort will emphasize the excitation of the required mode through the use of hybrid-junction feed assemblies, as indicated in Section 2.2, and the development of broadband components for use in the prototype model.

2.4.3 Spiral Phase Shifters

The application of the spiral antenna to a method of continuously variable phase shift lends itself to a compact and lightweight unit with low loss and relatively broad bandwidth capabilities.

For the purpose of this investigation, two spiral antennas designed to operate from 2.0 to 4.0 kmc were used. To excite the dominant mode of circular guide the spirals were placed face to face in a circular waveguide two feet long. Photographs are seen in Figures 20 and 21.

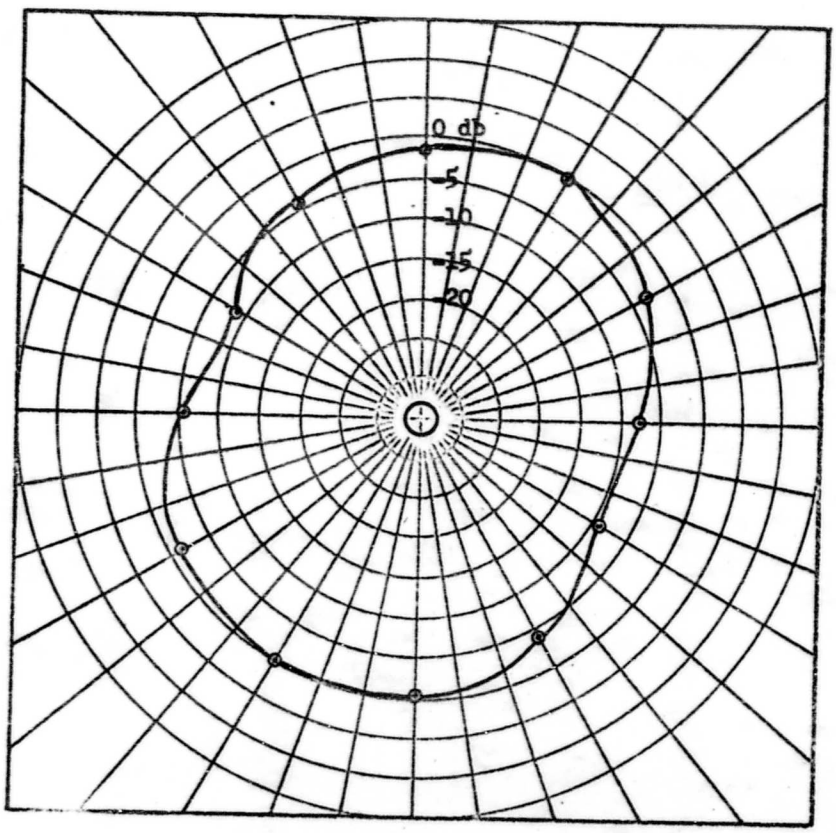

FIGURE 18. RELATIVE FIELD STRENGTH - FOUR PROBE UNIT

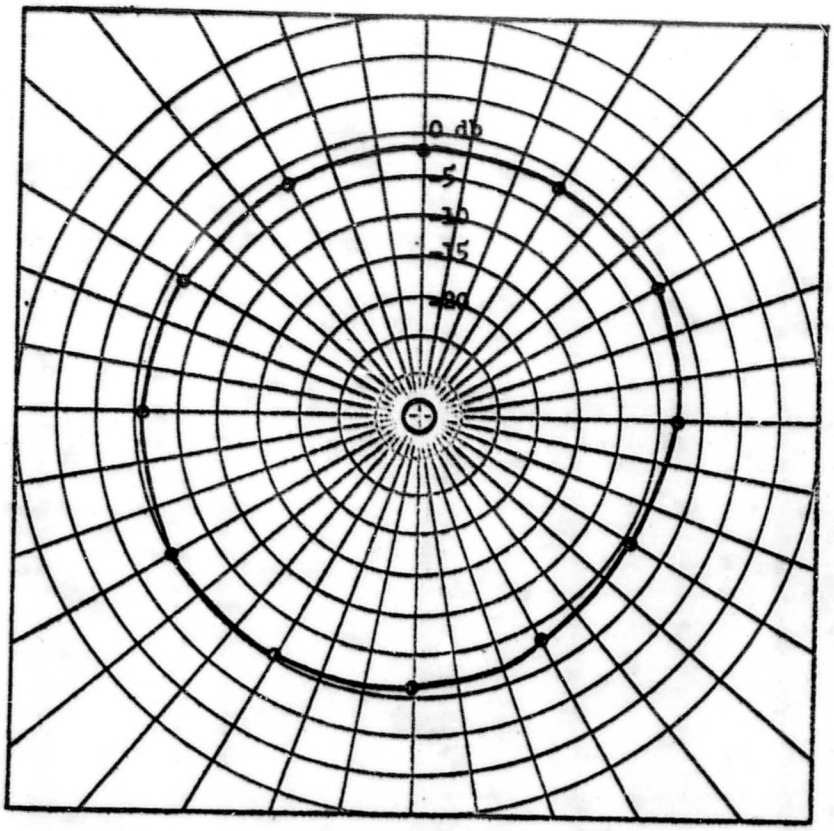

FIGURE 19. RELATIVE FIELD STRENGTH - FOUR PROBE UNIT

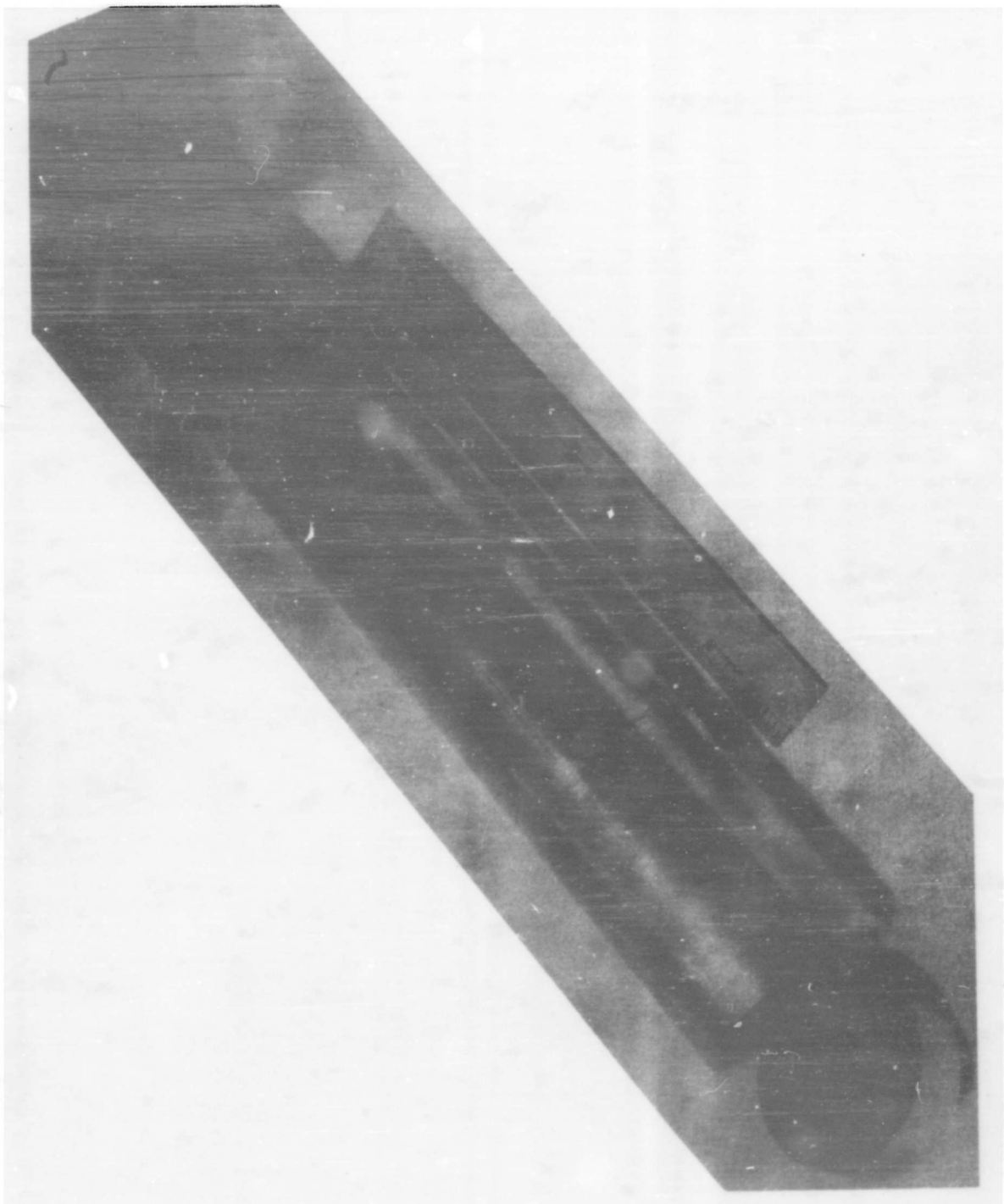

Figure 20. Spiral Phase Shifter.

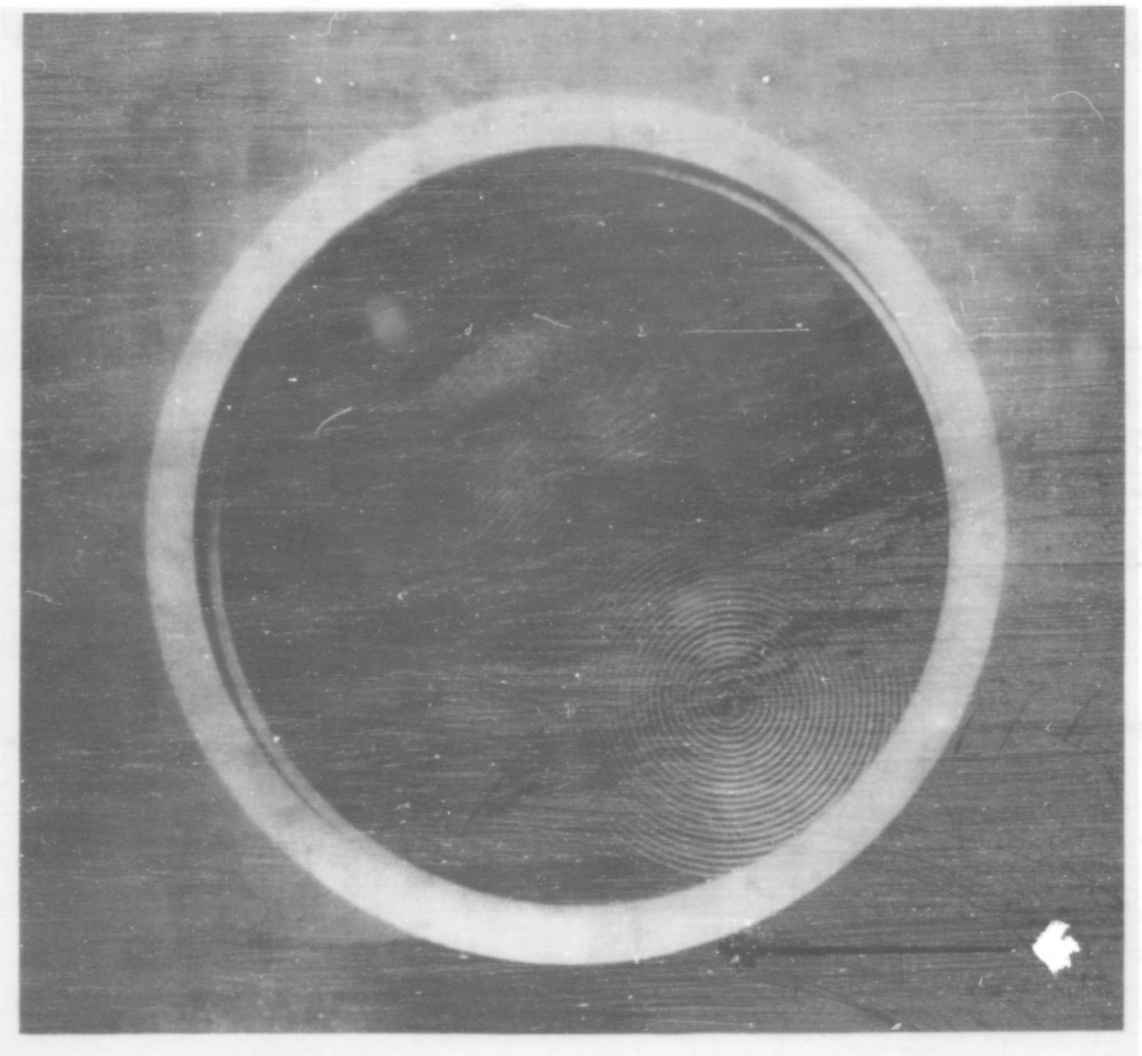

Figure 21. Spiral Antenna Mounted in Circular Waveguide.

The amount of loss associated with this device and the amount of phase shift which can be realized are dependent upon efficiency of the two antennas utilized and the axial ratio of the individual antennas.

The first step was the measurement of the input VSWR of the two antennas, which are shown in Figure 22. Although the measured VSWR is not as low as is theoretically possible, this parameter should affect only the loss figure associated with the phase shifter. No work was done at this point to improve the VSWR of these particular spiral antennas, but VSWR's of the order of 2:1 for a frequency band of an octave are easily attainable with this type antenna.

The axial ratios of the two antennas were measured and found to be of the order of 1.5 db over an octave of frequencies. A plot of these values of axial ratio will be found in Figure 23. These values of axial ratio can be lowered considerably by the proper choice of material on which the antenna is etched. A material such as teflon impregnated fiberglas provides best results.

Both spirals were then placed in the circular guide face to face. One was fed through a coaxial slotted-line and the other was mounted so as to terminate the circular guide. Holes were drilled 30 degrees apart around the guide for the purpose of accommodating a probe for measuring the purity of the mode excited in the guide.

A detector was placed on the receiving antenna with a standing-wave indicator to measure the WOW or variation in insertion loss of the system. A plot of these data is found in Figure 24.

The axial ratio of the spirals mounted in the guide was measured and it was found that the axial ratio was affected slightly when placed in the guide.

The test unit proved to be relatively small and compact. Because the antenna is being used to excite a circularly polarized field in a waveguide, the separation between elements is not controlled by or dependent upon the requirements for range as would be the case in the far field of the radiation pattern. Because this is the case, the overall length of the unit may feasibly be very short without degradation in performance.

Experimental measurements obtained thus far with the spiral phase shifter have been inconclusive because of the erratic nature of the data. Although the unit will be investigated further, the coaxial phase shifter will be given primary emphasis because of its more compact size. Furthermore, even though the spiral element is inherently very broadband, the cylindrical guide has a basic limitation of 1.4:1 imposed by the first higher order mode. The coaxial guide, on the other hand, has a bandwidth of approximately 2:1.

2.4.4 Two-Wire Line Phase Shifter

A two-wire line six feet long has been set up on a five foot square

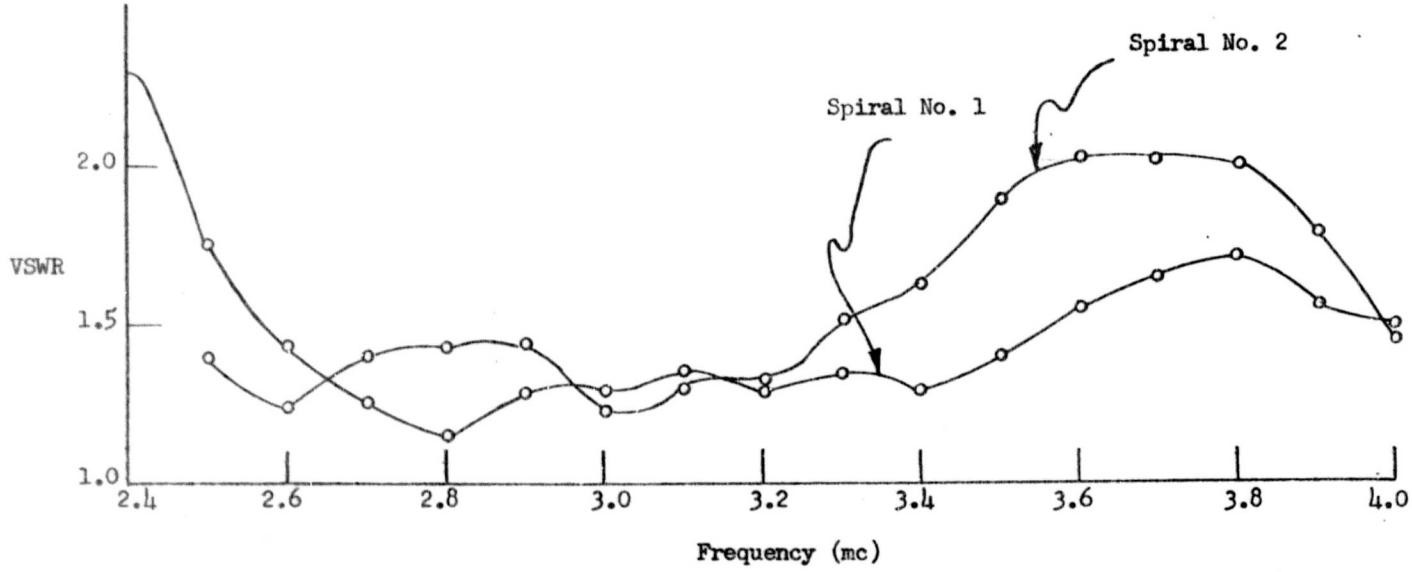

FIGURE 22. VSWR OF TWO SPIRAL ANTENNAS

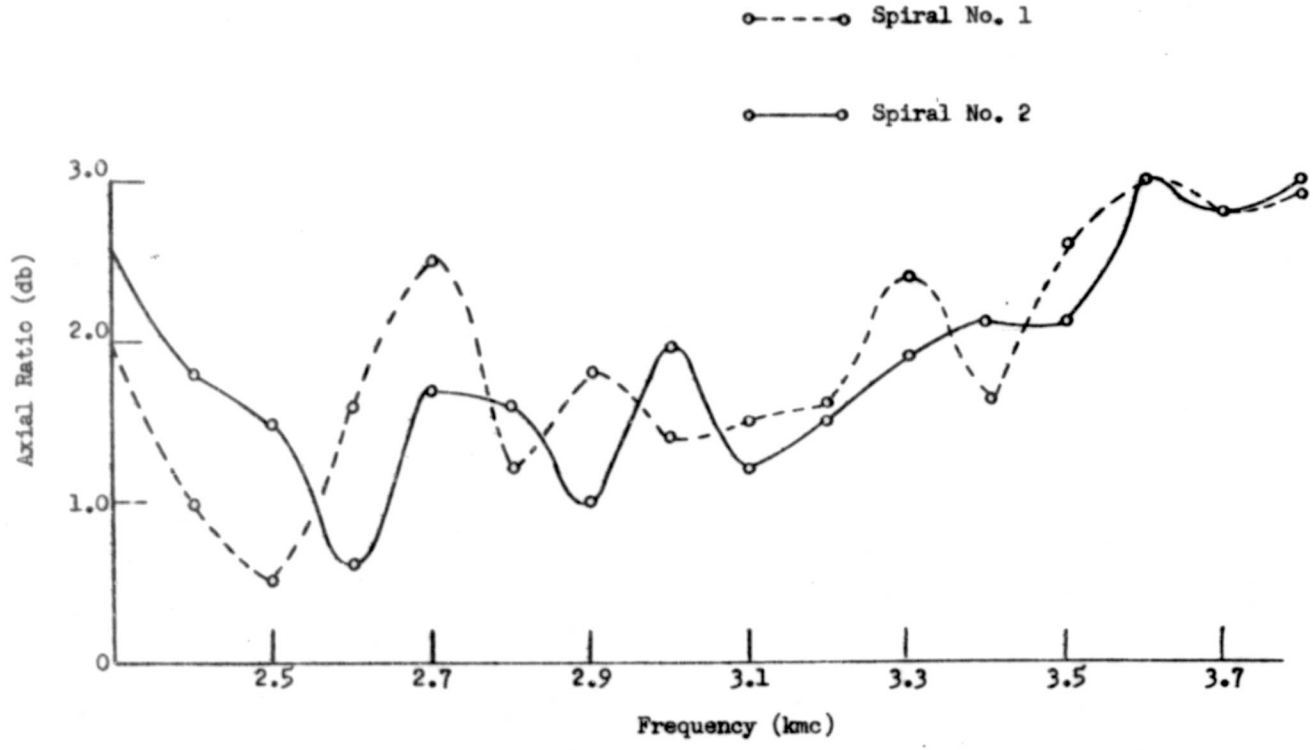

FIGURE 23. AXIAL RATIO OF TWO SPIRAL ANTENNAS

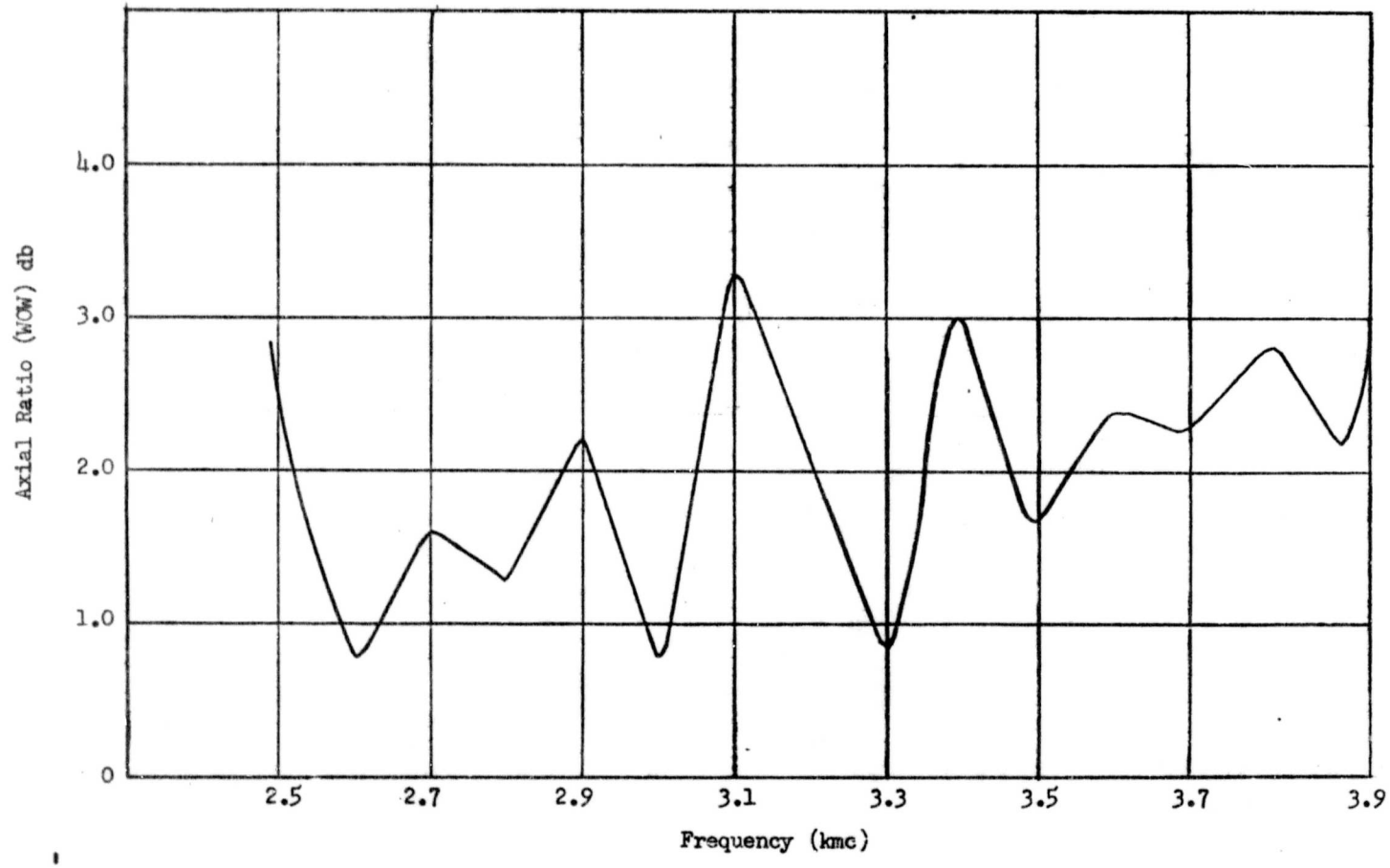

FIGURE 24. WOW OR VARIATION IN INSERTION LOSS

aluminum ground plane. The line is fabricated of 1/8 inch diameter brass rods and supported along its length by slotted plexiglass rods fastened to the ground plane. The feed arrangement consists of a coax to two-wire line balun for both the input and output terminals. Figure 25 shows the assembled line with an anisotropic dielectric cylinder inserted between the lines.

The two most feasible methods of producing a shift of phase in two-wire line are by use of capacitive plates on the line or by inserting a dielectric material either between the lines or mounted coaxially on the lines. These methods have been illustrated in Section 2.3.

In this report only the method involving use of the pin dielectric cylinder is undertaken. The pin dielectric to be used is similar to that described by Bowie and Chadwick[9]. The diameter of the cylinder is one inch; therefore, the two-wire line was set up to accept this size. The dimensions used in setting up the line were chosen so that the effect of the ground plane on the impedance of the line is negligible. The dimensions are as shown in Figure 9.

The most important factor in determining the impedance of the line is the ratio D/d.

When the line had been set up, a dipole and detector were used to determine if the line was radiating excessively or operating in other than the balanced mode. This check indicated that the maxima of the radiation from the line were greater than 40 db below the level of the input to the line. It was also determined that the line was operating in the balanced mode at 1000 mc. With the line set up as described, measurements were taken of the input VSWR and insertion loss of the line. Measured values of insertion loss are to include any radiation loss that might exist. Plots of these readings are found in Figure 26. The pin dielectric cylinder, which was made by casting a teflon/epoxy resin ($K = 2.2$, $\tan \delta = 0.005$) into a mold, was then inserted between the lines and input VSWR and insertion loss were measured for various spacings of the dielectric between the line. These data are found in Figure 27.

Figure 28 shows the preliminary data taken on phase shift for different spacings of the dielectric in the line and for angular rotation of the dielectric cylinder. These preliminary readings were taken using a slotted line at the input of the two-wire line to give an indication of phase shift. Final measurements will be taken using a probe and sliding carriage placed immediately below and between the line. This will give more accurate readings and will also allow measurement of the phase shift occurring in the region beyond the dielectric cylinder and in the area of the cylinder itself. It will be observed from the plots of insertion loss versus frequency that the line appears narrowbanded. Checks were made at those frequencies where the measured insertion loss was high to ascertain the cause for this loss. There was no noticeable increase in the level of radiation from the line at any point except the coax to two-wire line balun at the input terminal. It is felt that a portion of the loss may be due to the change in effect of the dielectric with changes in frequency. It is also interesting to note that the greatest degree of phase shift occurs when the center of the dielectric is slightly below the

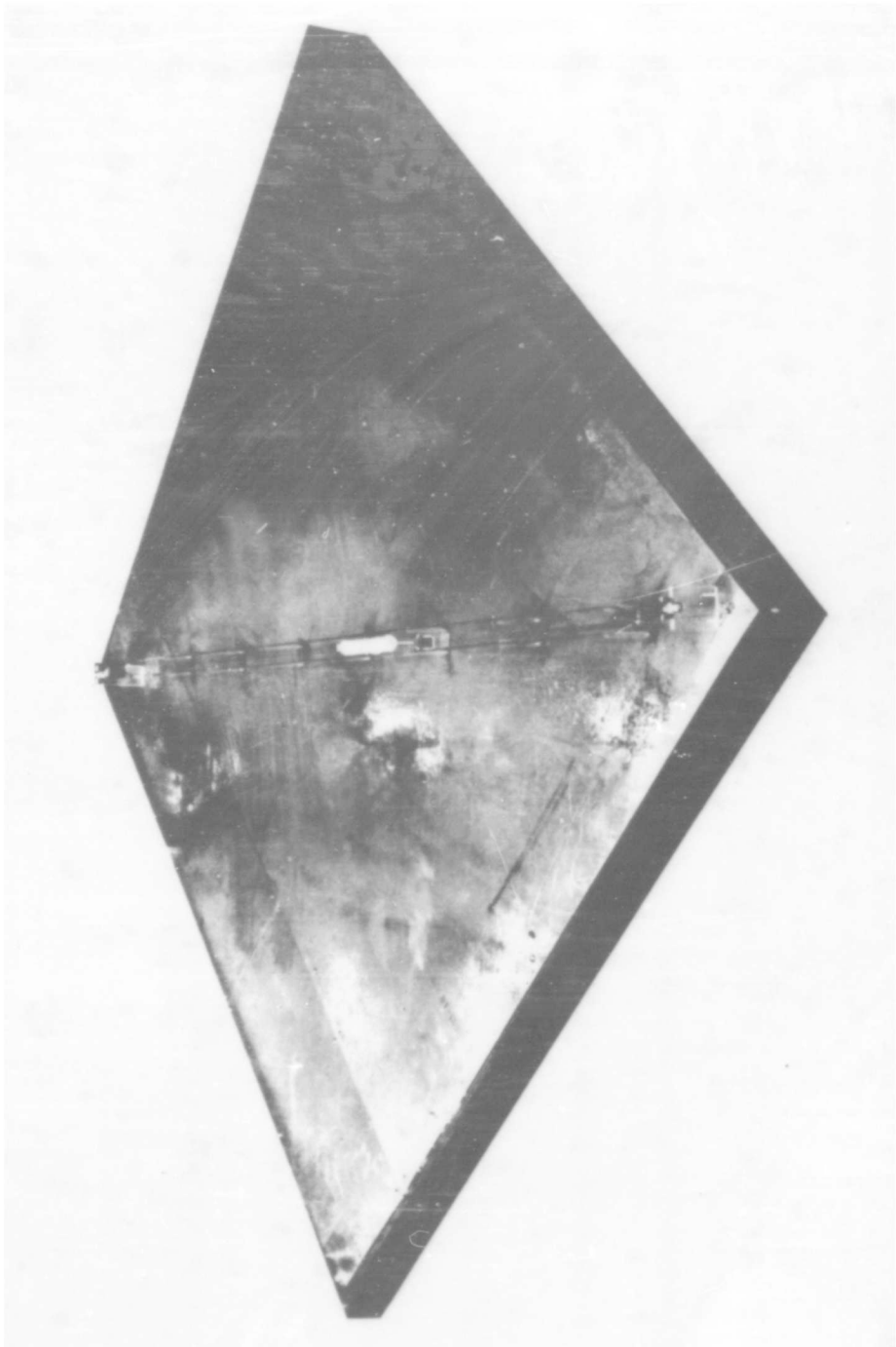

Figure 25. A Two-Wire Line.

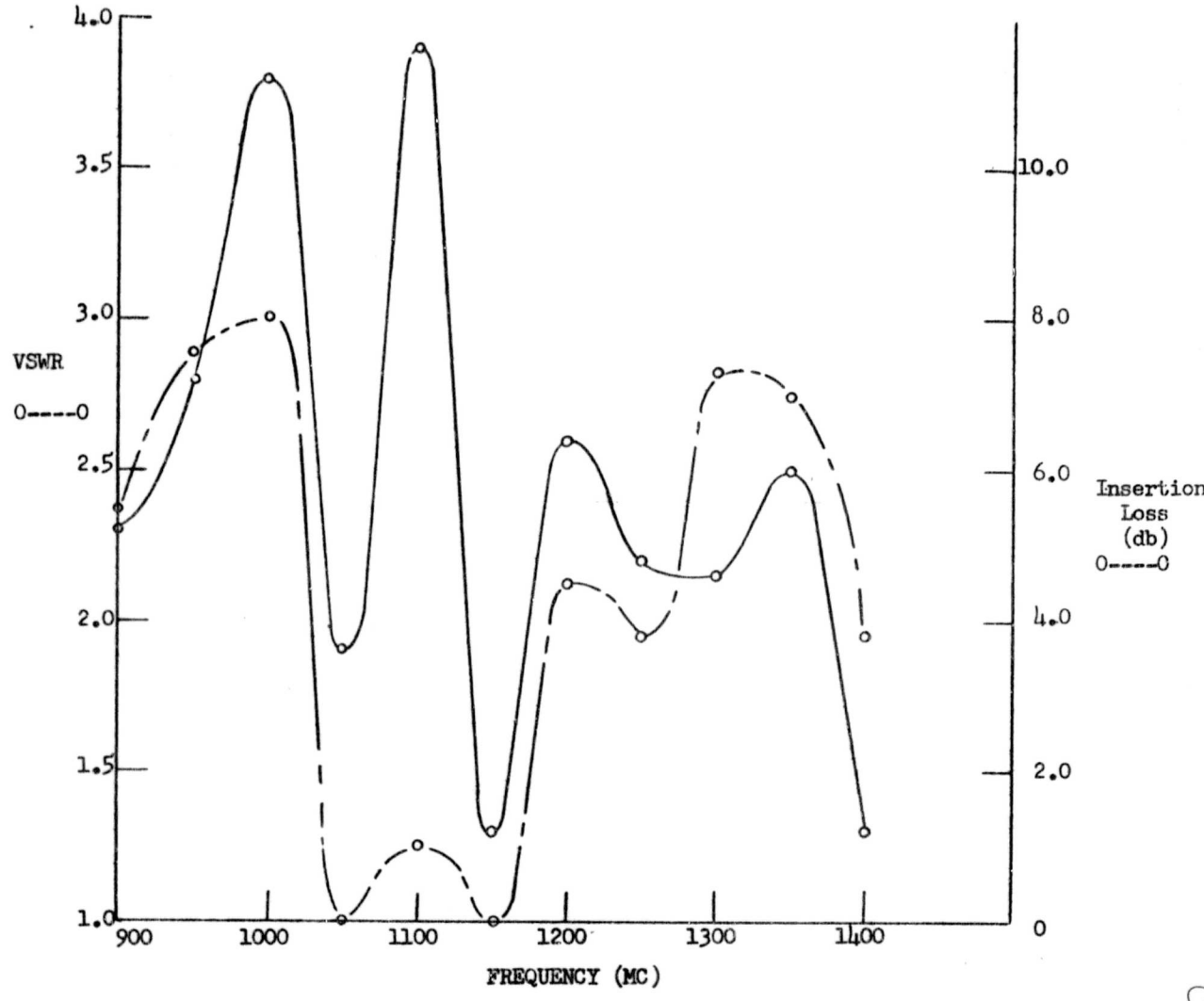

FIGURE 26. INSERTION LOSS - TWO-WIRE LINE

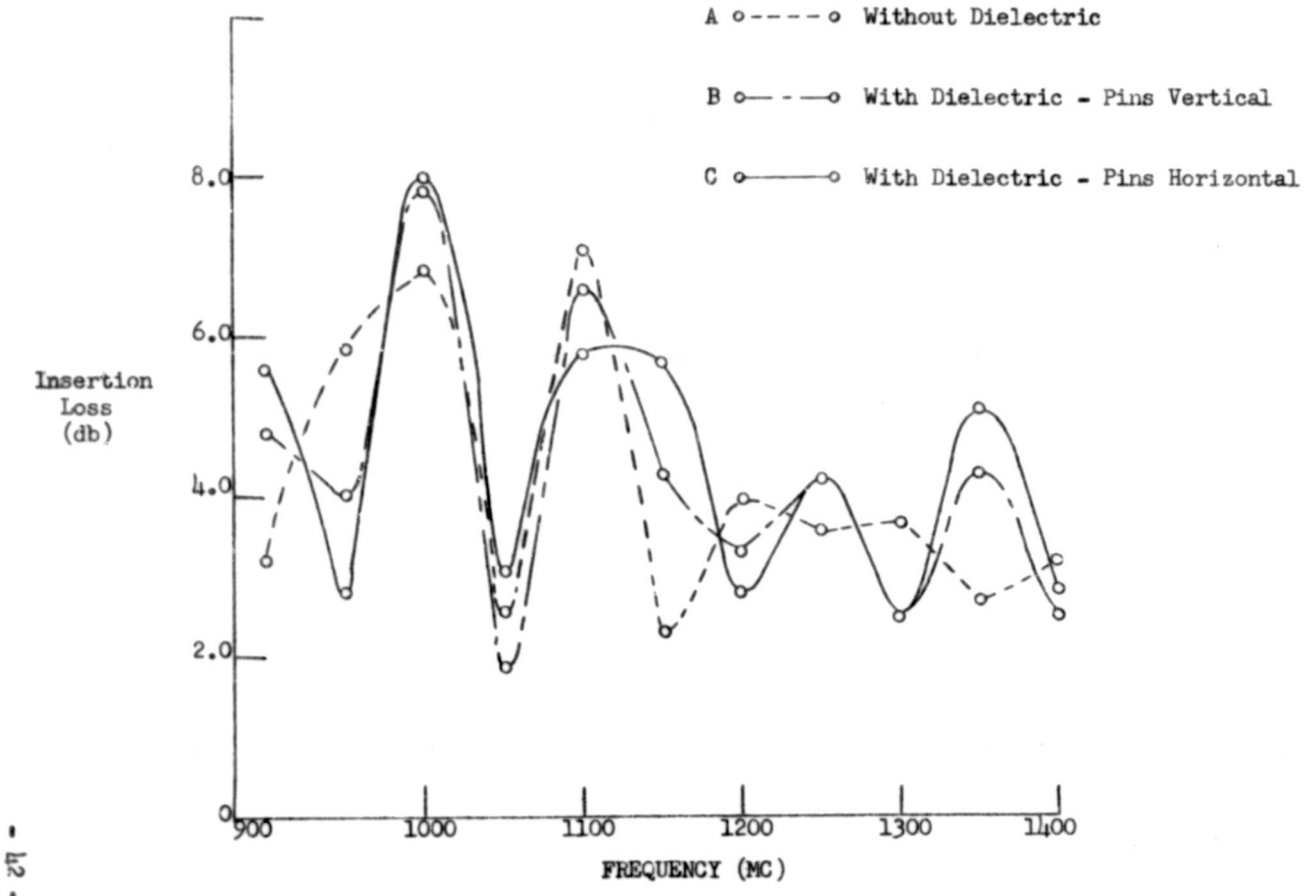

FIGURE 27. INSERTION LOSS AND VSWR - TWO-WIRE LINE WITH DIELECTRIC INSERTED.

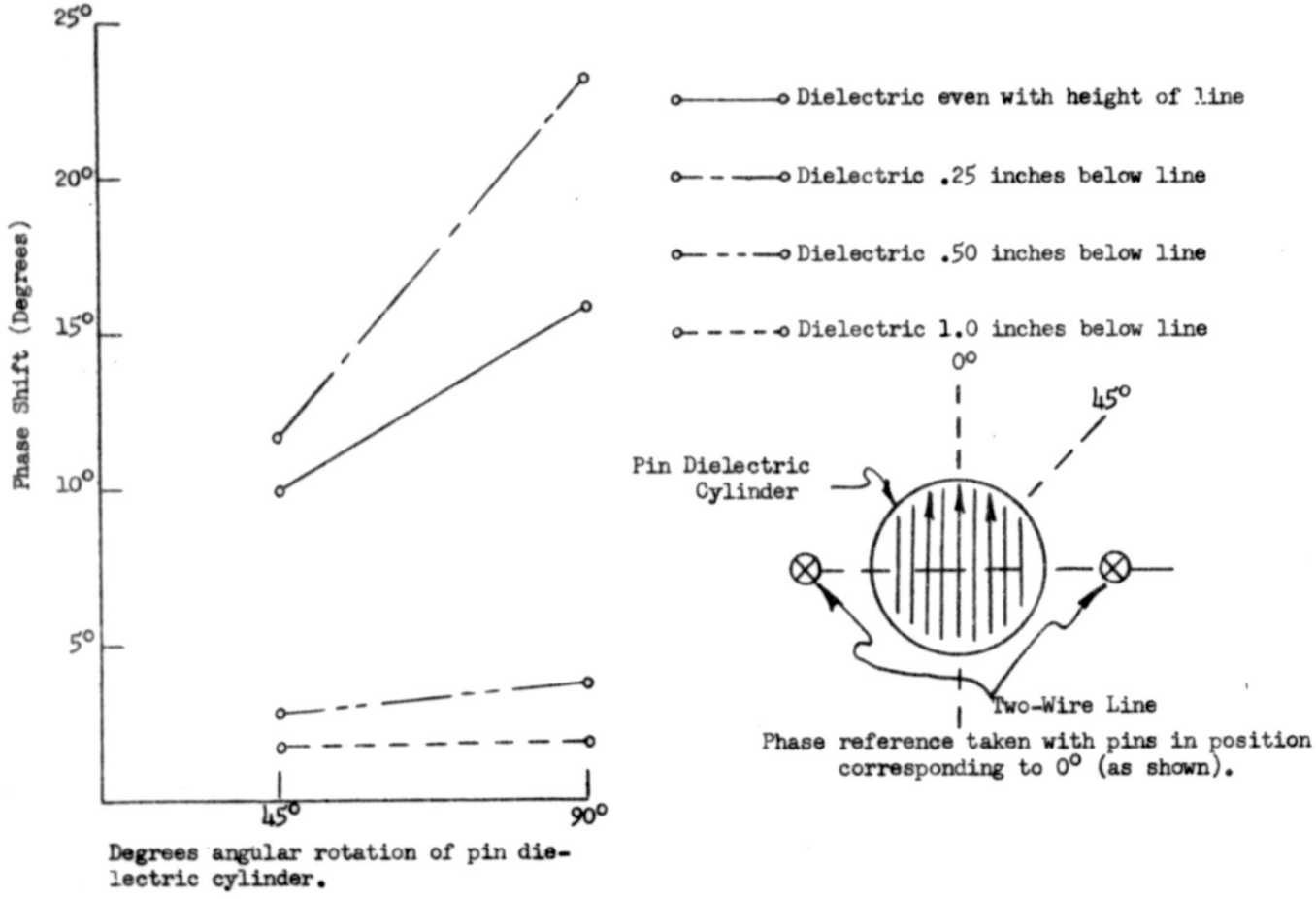

FIGURE 28. PHASE SHIFT VERSUS ROTATION AND PLACEMENT OF PIN DIELECTRIC IN TWO-WIRE LINE.

center of the two-wire line. Preliminary measurements indicate a phase shift of approximately 24 degrees in the length of line preceding the pin dielectric cylinder. A sliding carriage and probe were installed below the ground plane with the probe extending up through the ground plane under the two-wire line. Checks with this probe verified the measured phase shift in the region beyond the dielectric cylinder.

III. ELIMINATION OF BROADSIDE RESONANCE IN TRAVELING-WAVE ARRAY

The traveling-wave power distribution system, which couples off energy sequentially through matched directional or unmatched symmetrical junctions, is commonly used in exciting and scanning linear antenna arrays. Scanning can be achieved either by changing frequency or by introducing identical phase shifts in the interelement line sections.

If the junctions that couple energy from the transmission line to the radiating element are matched, as in the example of directional couplers, the input impedance is essentially independent of the beam position. If, however, the junctions are mismatched, as in waveguide slot arrays, the impedance exhibits a resonance as the beam is scanned through the broadside position, caused by the constructive addition of the reflected components from all the junctions.

The following paragraphs indicate a theoretical approach to the solution of the broadside resonance problem in traveling-wave arrays. The approach relies upon the assumption that the junction can be separated from the radiating element and that the primary source of reflection is the junction.

Simply stated, the resonance of the traveling-wave distribution structure is deadened by randomly varying the phase of the reflected components. The conventional system is shown in Figure 29(a). All interjunction line lengths are equal and all element line lengths are equal. The element line lengths are increased by various amounts Δ_n as shown in Figure 29(b). The changes in the interjunction lines required to maintain focusing of the array are also indicated. It is now easily seen that the broadside resonance can be eliminated, and if the increments Δ_n are selected with no systematic variation, that is, in a random fashion, the resonance cannot occur at any other beam position.

The problem of estimating the input impedance to the line when the conductances are randomly spaced can be approached in various manners. Although papers have dealt with the effects of random reflections, they have considered reactive rather than resistive discontinuities[11,12]. It is possible to assume either the addition of energy reflected or the addition of the conductances in a random fashion. The two relationships are

$$\left|\rho_{in}\right|^2 = \sum_{n=1}^{N} \left|\rho_n\right|^2 \quad \text{or} \quad \left|\rho_{in}\right| = \left[\sum_{n=1}^{N} \left|\rho_n\right|^2\right]^{1/2} \tag{3-1}$$

$$\left|Y_{in} - 1\right|^2 = \sum_{n=1}^{N} c_n^2 \tag{3-2}$$

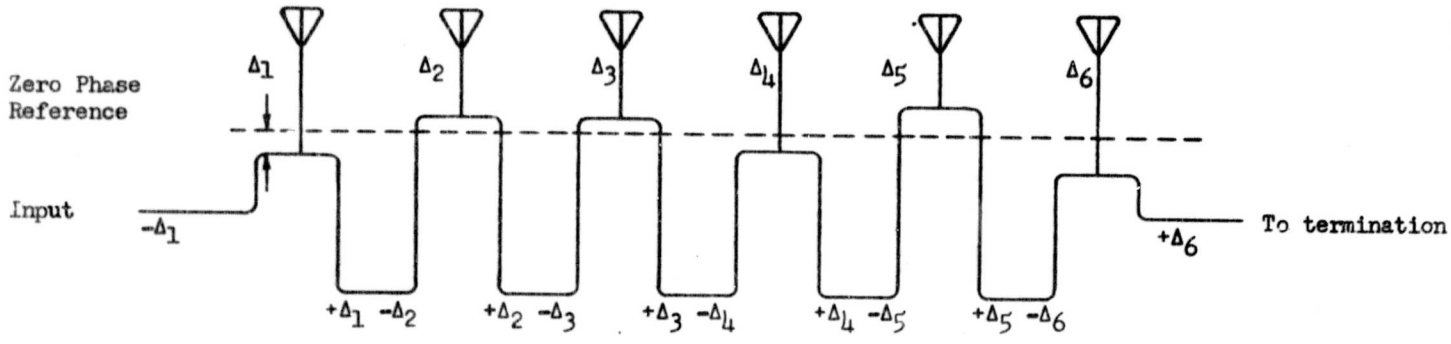

(b) Phase Staggered Coupling Junctions

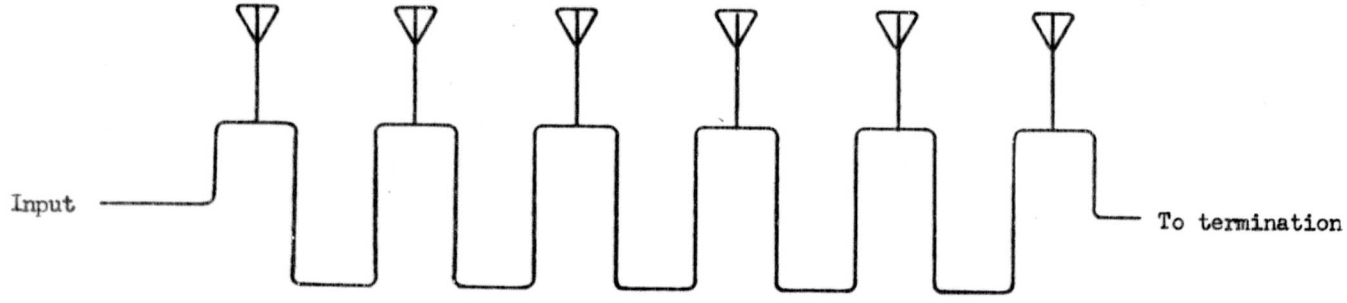

(a) Conventional Traveling-Wave Array

FIGURE 29. CONVENTIONAL AND IMPROVED TRAVELING-WAVE ARRAYS

where

ρ_{in} is reflection coefficient at input
ρ_n is reflection coefficient of nth junction
Y_{in} is input admittance
c_n is conductance of nth junction
N is number of junctions.

The approximations of Eqs. (3-1) and (3-2) hold for small ρ_n and c_n, as may be shown by the following development:

$$Y_n = 1 + c_n$$

$$\rho_n = \frac{1 - Y_n}{1 + Y_n} = \frac{-c_n}{2 + c_n} \approx -\frac{c_n}{2}$$

$$\sum_{n=1}^{N} |\rho_n|^2 = \sum_{n=1}^{N} c_n^2 ,$$

and the agreement can be shown by finding the input VSWR, S, from Eq. (3-2) and relating ρ_{in} to S.

$$|Y_{in} - 1| = \left[\sum_{n=1}^{N} c_n^2 \right]^{1/2} \qquad (3\text{-}3)$$

$$S = (Y_{in})_{max} = 1 + \left[\sum_{n=1}^{N} c_n^2 \right]^{1/2}$$

$$|\rho_{in}| = \frac{S - 1}{S + 1} = \frac{\left[\sum_{n=1}^{N} c_n^2 \right]^{1/2}}{2 + \left[\sum_{n=1}^{N} c_n^2 \right]^{1/2}}$$

$$= \frac{2\left[\sum_{n=1}^{N} |\rho_n|^2 \right]^{1/2}}{2 + 2\left[\sum_{n=1}^{N} |\rho_n|^2 \right]^{1/2}}$$

$$|\rho_{in}| = \frac{\left[\sum_{n=1}^{N} |\rho_n|^2 \right]^{1/2}}{1 + \left[\sum_{n=1}^{N} |\rho_n|^2 \right]^{1/2}}$$

Thus, Eqs. (3-1) and (3-2) agree so long as $\sum_{n=1}^{N} |\rho_n|^2$ is small, which may

not always be the case. Equations (3-2) and (3-3) are selected as a more desirable approximation because they can never give the impossible result of a reflection coefficient greater than unity.

Two important design aspects of the traveling-wave array are the maximum allowable conductance and the energy dissipated in the load. These are related to the sum of all conductances as follows:

$$\sum_{n=1}^{N} c_n = A$$

$$\bar{c}_n = \frac{A}{N} \approx 1/2\left(\frac{1}{N} + c_{max}\right)$$

assuming that the first conductance is approximately 1/N and the last is c_{max}, and that the conductances taper approximately linearly. Thus,

$$c_{max} \approx \frac{2A - 1}{N}$$

$$\text{or} \qquad A \approx 1/2(c_{max} N + 1). \tag{3-4}$$

The energy in the load is limited by c_{max} and the excitation of the last element:

$$\frac{P_N}{P_L} = c_{max} \tag{3-5}$$

$$P_N = \frac{a}{N} \tag{3-6}$$

where

P_N is energy in Nth element
P_L is energy in load
a is determined by illumination taper -- $a = 1$ for uniform; $a < 1$ for tapered illumination.

Equations (3-5) and (3-6) may be combined to give

$$P_L = \frac{a}{N c_{max}} . \tag{3-7}$$

The input VSWR can be expressed in terms of A or the other relationships

$$S = 1 + \left[\sum_{n=1}^{N} c_n^2\right]^{1/2}$$

$$\approx 1 + \left[\frac{NA^2}{N^2}\right]^{1/2} = 1 + \frac{A}{\sqrt{N}}$$

$$= 1 + \frac{\sqrt{N}}{2}\left(\frac{1}{N} + c_{max}\right) .$$

Results are calculated for a simple example to give a rough indication of the effectiveness of this procedure in improving input impedance. A uniform distribution is assumed for an array of 80 elements using a maximum conductance of 0.1. For this case $a = 1$ and the energy dissipated in the load is 12.5 per cent. The estimated VSWR is found to be approximately 1.5, whereas the VSWR at broadside resonance is approximately 5.4.

It is now of interest to consider some of the uses to which this feed system can be put. In some applications it is desirable to make maximum use of the scan capability of the array by switching the input from one end to the other. Aside from the problem of aperture distribution that is introduced by coupling to the elements from two directions, there remains the problem of eliminating the broadside resonance for each input. Reference to Figure 30 shows that the line length errors introduced by using the line in the opposite direction are as follows:

Element	Phase Error
6	$+2\Delta_6$
5	$+2\Delta_5$
4	$+2\Delta_4$
3	$+2\Delta_3$
2	$+2\Delta_2$
1	$+2\Delta_1$

or in general $\Delta l_n = 2\Delta_n$. Thus, if the Δ_n were originally chosen to provide phase cancellation of reflected components, the aperture distribution obtained by feeding in the opposite direction also possesses random phase, making focusing impossible.

Although this result discourages the feeding of a phase-staggered array from both ends, it does allow a constructive application for the single-input configuration: the termination that is usually located at the end of the traveling-wave array to absorb approximately five or ten per cent of the input energy can be eliminated, since the reflected wave will not be focused. The effect of the reflected wave will be to add side lobes of fairly low magnitude. If it is assumed that the reflected wave radiates essentially omnidirectionally, its level is below isotropic by the amount that the traveling wave is attenuated in its passage through the array. If the gain of the array is roughly N, the sidelobe level introduced by the reflected wave is

$$G_s \approx P_L/N$$

which is 28 db for the example used above.

IV. MULTIPLE BEAMS FROM LINEAR ARRAYS

4.1 Introduction

The array-type antenna was in use many years before adoption of the microwave optics techniques for forming directive beams. However, it had only a limited number of elements and seldom, if ever, produced more than a single directive beam simultaneously. The microwave optics techniques, on the other hand, provided capability for large apertures and were adaptable to producing multiple beams. Since, in many applications, the array has advantages over the microwave optics counterpart, it is desirable to develop techniques permitting the use of a large number of array elements and providing multiple beams from such an array.

The microwave optics systems were those capable of yielding wide-angle performance. The inputs to this system were simple feed horns. Many different techniques were employed. The early units consisted of parabolic reflectors with large F/D ratios. Later work involved Schmidt systems, Luneberg lenses and the parabolic torus reflector.

In all of the systems, with the exception of the Luneberg lens, some phase error existed in the apertures forming the majority of the beams. In general, the wide-angle capability of the system, or the number of multiple beams which the system could produce, was limited by this inherent phase error. Since the Luneberg lens showed the most promise, it was found that this structure, or some related configuration, would be most desirable for achieving multiple beams.

It is well known that all microwave optics structures employ a feed and focusing objective. In such a system, inefficiency is introduced due to spill-over of energy from the feed which is not captured by the objective. A more serious problem has been a decreased aperture efficiency, due to the requirement that the multiple beams cross-over at a very high level. If levels as high as 3 db are required, problems in isolation among the various elements are introduced. This is particularly severe with regard to the isolation between an element and its neighbors. Variations in the impedance match in neighboring feeds can drastically affect the radiated beam associated with a given feed.

Considerations of efficiency, beam overlap, and element isolation indicate the difficulties that are encountered in obtaining a microwave optics system producing multiple beams. Since the work done on obtaining multiple beams from an array has, to the greatest extent, involved complex feed structures employing active elements, it is desirable to consider the problem anew and to determine how this might be achieved entirely with a passive transmission-line network, so that the antenna system is capable of both transmitting and receiving with a minimum of complexity. The remaining sections of this report describe techniques that have been evolved for utilizing passive networks capable of associating N inputs with N elements to produce N-multiple beams.

Research on multiple-beam arrays is in progress at the W. L. Maxson Corporation with significant results.[13] The approach used, however, although simpler in geometry, consists basically of traveling-wave arrays and is inherently somewhat inefficient. The purpose of the next sections is to explore the fundamental limitations on multiple-feed systems before giving detailed attention to design aspects.

4.2 Multiple-Beam Pattern Characteristics

Before the problem of realizing the multiple-feed system is considered, it is necessary to evaluate the multiple-beam radiation pattern characteristics that are attainable from a linear array. It would be desirable to find the relationships among beam spacing and aperture distribution with its associated aperture efficiency, beamwidth, and side lobe level.

The desirable feed network would be one in which the array attains maximum effective aperture for every angle of incidence; that is, the feed system would be matched as seen from both the inputs and from the elements.

The problem of beam spacing is best approached by considering the case of the uniform distribution, a typical array factor of which is shown in Figure 30 for a six-element array. Array or space factors are expressed in terms of ψ, the relative phase of adjacent elements, which can easily be converted to angle in any specific application with the equation $\psi = (2\pi d/\lambda) \sin \theta$. It can be seen that the nulls are evenly spaced, so that six beams can be overlapped without repetition, the maxima being located at the nulls of the other beams. Any other location of the beams would mean reduced aperture efficiency, since the uniform distribution should be 100 per cent efficient. On this basis there should be one beam for each element of the array, and the beams are spaced $2\pi/N$ in ψ, where N is the number of elements.

The question now is whether it is possible to use the same spacing for distributions other than uniform. The situation can be analyzed in terms of the individual components of the array factor. The most general case is the one in which the element distribution is in phase but the amplitudes are arbitrary. If the amplitudes are denoted by $a_1, a_2 \ldots a_N$, the distribution can be broken down into even and odd components, the even distribution being

$$\frac{a_1 + a_N}{2}, \quad \frac{a_2 + a_{N-1}}{2}, \quad \frac{a_3 + a_{N-2}}{2} \quad \ldots\ldots$$

and the odd being

$$\frac{a_1 - a_N}{2}, \quad \frac{a_2 - a_{N-1}}{2}, \quad \frac{a_3 - a_{N-2}}{2} \quad \ldots\ldots$$

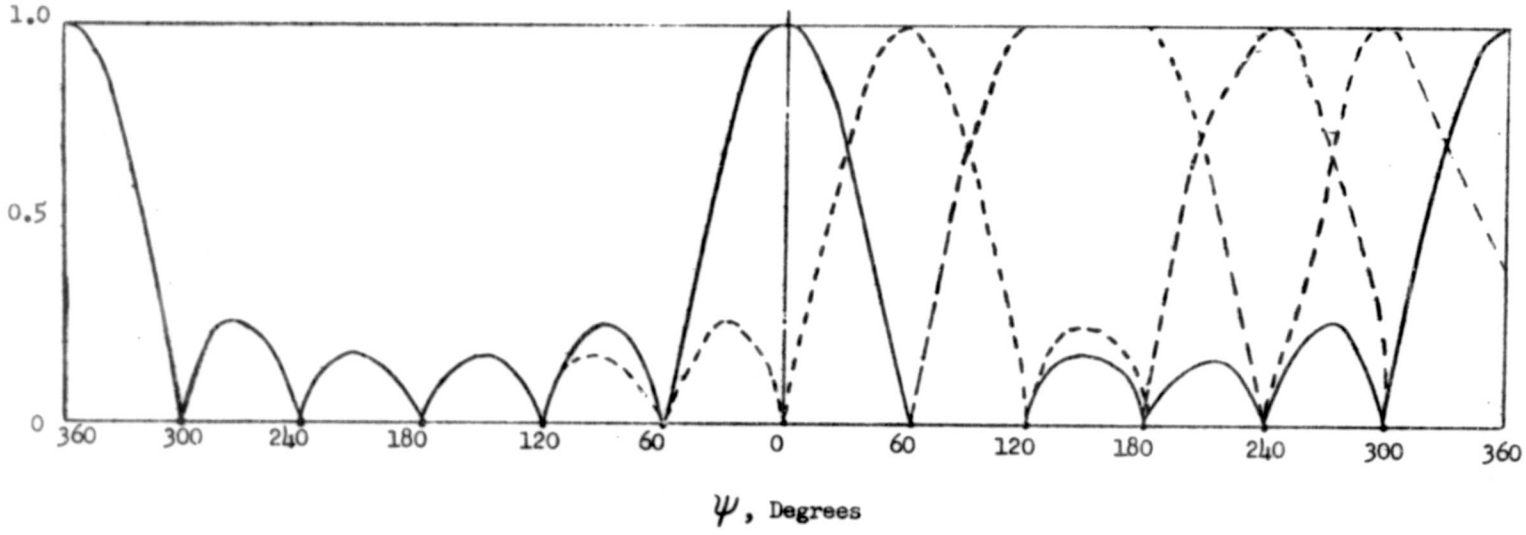

FIGURE 30. OVERLAPPING ARRAY FACTORS FOR UNIFORM SIX-ELEMENT ARRAY

The array factors can be written

$$E_e(\psi) = (a_1 + a_N)\cos(N-1)\psi/2 + (a_2 + a_{N-1})\cos(N-3)\psi/2 + \ldots.$$

$$j\,E_o(\psi) = (a_1 - a_N)\sin(N-1)\psi/2 + (a_2 - a_{N-1})\sin(N-3)\psi/2 + \ldots.$$

Since the even and odd array factors are in phase quadrature, the power pattern can be written as the sum of their squares,

$$P(\psi) = E_e^2(\psi) + E_o^2(\psi).$$

$$E_e^2(\psi) = (a_1 + a_N)^2\cos^2(N-1)\psi/2 + 2(a_1 + a_N)(a_2 + a_{N-1})\cos(N-1)\psi/2 \times \cos(N-3)\psi/2 + (a_2 + a_{N-1})^2\cos^2(N-3)\psi/2 + \ldots.$$

$$E_o^2(\psi) = (a_1 - a_N)^2\sin^2(N-1)\psi/2 + 2(a_1 - a_N)(a_2 - a_{N-1})\sin(N-1)\psi/2 \times \sin(N-3)\psi/2 + (a_2 - a_{N-1})^2\sin^2(N-3)\psi/2 + \ldots.$$

Straightforward trigonometric manipulation yields expressions of the following form:

$$E_e^2(\psi) = \frac{a_1 + a_N}{2}^2 + \frac{a_2 + a_{N-1}}{2}^2 + \ldots.$$

$$+ b_1\cos(N-1)\psi + b_2\cos(N-2)\psi + \ldots.$$

$$E_o^2(\psi) = \frac{a_1 - a_N}{2}^2 + \frac{a_2 - a_{N-1}}{2}^2 + \ldots.$$

$$+ c_1\cos(N-1)\psi + c_2\cos(N-2)\psi + \ldots.$$

Thus, the power pattern assumes the form

$$P(\psi) = a_1^2 + a_2^2 + \ldots. a_N^2$$

$$+ d_1\cos(N-1)\psi + d_2\cos(N-2)\psi + \ldots. \qquad (4\text{-}1)$$

As we shift from beam to beam, the variable ψ used in the above equations is altered by the appropriate phase, which may be written $m\,\phi$, where m is integral from one to the total number of beams M (not necessarily equal to the number of elements N). In order to insure a generally symmetrical phase distribution and beam coverage, $\phi = 2\pi/M$. For optimum coverage by the array, it is required that

$$\sum_{m=1}^{M} P(\psi, m) = \text{constant}.$$

Referring to Eq. (4-1) and inserting the appropriate phases, the expression for the total power radiated in a direction ψ by all beams can be written,

$$\sum_{m=1}^{M} P(\psi, m) = M(a_1^2 + a_2^2 + \ldots + a_N^2)$$
$$+ d_1 \sum_{m=1}^{M} \cos (N-1)(\psi + m\tfrac{2\pi}{M})$$
$$+ d_2 \sum_{m=1}^{M} \cos (N-2)(\psi + m\tfrac{2\pi}{M})$$
$$\ldots\ldots$$
$$+ d_n \sum_{m=1}^{M} \cos (\psi + m\tfrac{2\pi}{M}) \qquad (4\text{-}2)$$

Now, the periods of the arguments, $(N-1)\psi$, $(N-2)\psi$ .... , in Eq. (4-2) are $2\pi/N-1$, $2\pi/N-2$, ... 2π, while the change in the variable ψ introduced by traversing from one beam to another is $2\pi/M$. If the period coincides with the change in ψ for any component, then the sum for that component will be nonzero and a function of ψ. Obviously,

$$\sum_{m=1}^{N-1} \cos\left[(N-1)\psi + m2\pi\right] = M \cos\left[(N-1)\psi\right], \text{ and}$$

$$\sum_{m=1}^{N} \cos\left[(N-1)(\psi + m\tfrac{2\pi}{N}\right] = 0, \text{ for example.}$$

Thus, M cannot fall in the range one through N-1, and must assume the value N as was the case with the uniform array. It is, therefore, seen that the number of beams or over-all radiating efficiency of the aperture is independent of the illumination. An interesting result is that as the side lobes are reduced and the beamwidth broadens, the beam crossover level becomes higher for two reasons. First, the aperture efficiency of the individual beam decreases, so that relative crossover can easily increase. Second, the lower side lobe characteristic results in less received energy distributed to other inputs, so that the absolute crossover can also be expected to increase some before too much gain is lost.

4.3 Limitations on the Feed Network

The previous discussion had as its starting point the assumption of a given aperture distribution, with appropriate phase characteristics for the multiple-beam radiation pattern coverage. No consideration was given to the realizability of the network required to connect the array elements with the inputs so as to provide the assumed aperture distributions.

A diagram of the network inputs and outputs is shown in Figure 31. If it is required that the transmission loss from an input to the outputs to the elements be zero and that the inputs be isolated from one another, the scattering matrix is of the following form:

$$\begin{bmatrix} 0 & 0 & \cdots & 0 & S_{1\,N+1} & S_{1\,N+2} & \cdots & S_{1\,2N} \\ 0 & 0 & \cdots & 0 & S_{2\,N+1} & S_{2\,N+2} & \cdots & S_{2\,2N} \\ \vdots & \vdots & & \vdots & \vdots & \vdots & & \vdots \\ 0 & 0 & \cdots & 0 & S_{N\,N+1} & S_{N\,N+2} & \cdots & S_{N\,2N} \\ S_{N+1_1} & S_{N+1_2} & \cdots & S_{N+1_n} & 0 & 0 & \cdots & 0 \end{bmatrix}$$

The upper left quadrant indicates that the inputs are matched and isolated. The upper right and lower left quadrants represent transmission coefficients between the inputs and outputs, and the lower right quadrant is the reflection and transmission coefficients among the outputs to the array, as yet undetermined.

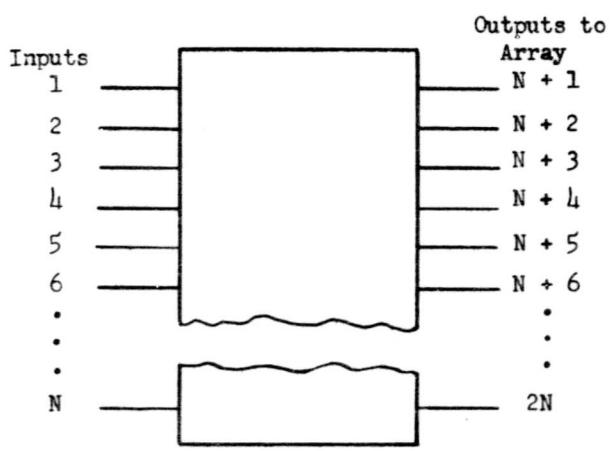

Figure 31. General 2N-Port Network for Mutiple-Beam Application.

It has recently been pointed out that the length (the sum of the squares of the magnitudes) of any row or column of a scattering matrix must be less than or equal to unity. In view of this limitation, the maximum transfer coefficient for amplitude distributions differing only in phase is given by

$$\sum_{b=1}^{N} \left|S_{ab}\right|^2 = N \left|S_{ab}\right|^2 \leq 1$$

$$\left|S_{ab}\right| \leq 1/\sqrt{N}. \qquad (4\text{-}3)$$

Since some transfer coefficients must be greater than $1/\sqrt{N}$ in a tapered distribution, Eq. (4-3) forces the conclusion that any tapered distribution is achieved only at the expense of net transmission loss from inputs to outputs. Thus, the feed system for uniform illumination is the only lossless one, so far as achieving maximum array efficiency is concerned.

Of course, if the feed system were to have fewer inputs than the number of elements in the array, Eq. (4-3) would be altered to read

$$S_{ab} \leq 1/\sqrt{P}, \quad P < N$$

where P is the number of inputs. In this event the assumptions of Section II concerning coverage by the array factors and number of beams from a given array would be violated.

Although it appears that efficient feed networks giving tapered illuminations may be realized at the expense of over-all beam coverage, such possibilities will not be further investigated at this time, and the following sections are devoted to feed networks connecting N inputs to N elements with uniform illumination.

4.4 Synthesis of Multiple-Feed Networks

The required microwave network has 2n ports and is matched at all ports. The n outputs on one side of the network that are excited by any of the n inputs on the other side possess a progressive phase characteristic that is a function of the input.

The first step is to determine just what phase characteristic is required. It is possible to select any 360-degree portion of the ψ coordinate in which to place the beams. Referring to Figure 30, the problem can be reduced to whether a beam maximum or a crossover point should be located at $\psi = 0$. If the feed system is to be symmetrical, it is preferable to locate the beams symmetrically, with a crossover point at zero. On the other hand, such an arrangement results in excessive backlobes from the outermost beams due to the second-order maximum which is beginning to form. These two beams can be discarded, or if the patterns were shifted so that one is located at $\psi = 0^\circ$ and one at $\psi = +180^\circ$ with a beam split between the edges of the coverage region, then only the split pattern need be discarded. These problems can best be dealt with when the practical design is undertaken. For present purposes, it is best to locate the beams with the symmetry corresponding to that expected of the multiple-feed network.

On this basis, the required phase relationships are as shown below. For six elements, the successive element phases are seen to be $\pm 30^\circ$, $\pm 90^\circ$, $+150^\circ$.

Element	1	2	3	4	5	6
Phase	0°	$\pm 30^\circ$	$+ 60^\circ$	$+ 90^\circ$	$+120^\circ$	$+150^\circ$
	0°	$\pm 90^\circ$	$\pm 180^\circ$	$\pm 270^\circ$	$\pm 360^\circ$	$\pm 450^\circ$
	0°	$\pm 150^\circ$	$\pm 300^\circ$	$\pm 450^\circ$	$\pm 600^\circ$	$\pm 750^\circ$

The solution will be shown to depend upon building blocks, the simplest of which is the hybrid junction. The hybrid junction is a building block because it can provide two overlapping beams from a two-element array, as shown in Figure 32a. It should be noted that there are various configurations which provide hybrid operation. Hybrids that rely on symmetry, such as the magic tee and ring hybrid, have in-phase and out-of-phase outputs. Directional-coupler hybrids have outputs that are 90 degrees out of phase. Some couplers give a phase lag to the coupled arm and some phase lead. In the following discussion the hybrid junction is a phase-lag coupler. Similar techniques would be applicable for use with the other components.

A single hybrid junction supplies rudimentary multiple-beam operation from a two-element array. The significance of the element, however, lies in its use as a building block for arrays with more elements and beams. Figures 32b and 32c indicate feed systems for four and eight elements, respectively, and the pattern for extending the number to any power of two is clear. The critical aspects of the arrangements are the interconnections among the hybrids and to the elements and the added phase shifts. All transmission lines in a given cross section are assumed equal in length except for the phase shifters.

The principal limitation on the use of hybrids is the restriction of the number of elements to powers of two. The alternative to this difficulty would be to find more building blocks. The next larger building block would be one in which three inputs and outputs are connected so that three beams could be obtained from a three-element array. This case is treated in Appendix A. Such a component consists of three lines equally coupled to one another so as to effect equal power division, followed by a 120-degree phase shifter on the output that will feed the central element.

An additional limitation on the use of small building blocks is the great number that are required to feed large arrays. For this reason a network of four inputs and four outputs is desirable, although it does not introduce any further flexibility in the number of elements. The derivation for such a junction is given in Appendix B and it is shown that only coupling mechanisms similar to those available in waveguide are applicable to this network.

Although junctions with greater numbers of inputs and outputs may be possible, no effort has been made to find them because of the discouraging prospects of a trial-and-error approach.

Listed below are the arrays with elements up to the number 128 that are available, with information on the number of hybrids required.

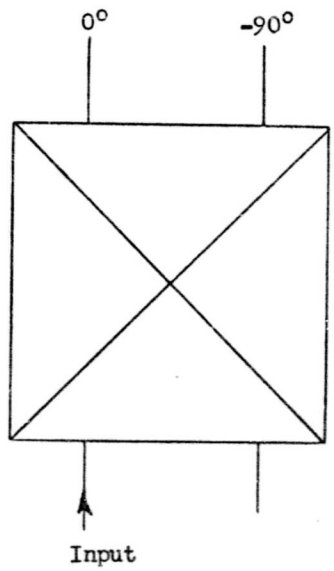

(a) Operation of Hybrid Coupler

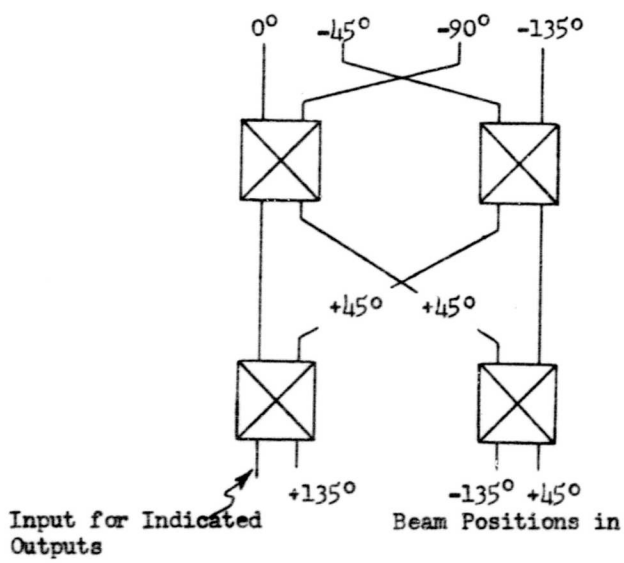

(b) Four-Element Feed System.

Figure 32. Hybrid-Coupler Multiple-Feed Systems.

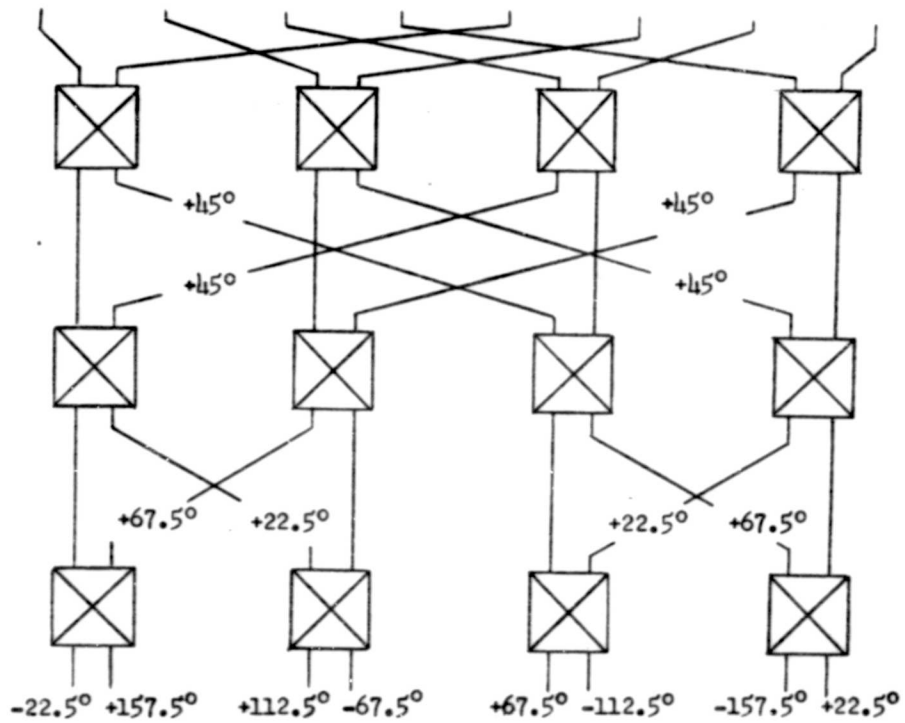

Beam Positions in Ψ

(c) Eight-Element Feed System

FIGURE 32c. HYBRID-COUPLER MULTIPLE-FEED SYSTEMS

Number of Elements $N = 2^l 3^m 4^n$	l	m	n	2 x 2 Hybrids	3 x 3 Junctions	4 x 4 Junctions	Total Junctions
2	1	0	0	1	0	0	1
3	0	1	0	0	1	0	1
4	0	0	1	0	0	0	1
6	1	1	0	3	2	0	5
8	1	0	1	4	0	2	6
9	0	2	0	0	6	0	6
12	0	1	1	0	4	3	7
16	0	0	2	0	0	8	8
18	1	2	0	9	12	0	21
24	1	1	1	12	8	6	26
27	0	3	0	0	27	0	27
32	1	0	2	16	0	16	32
36	0	2	1	0	24	9	33
48	0	1	2	0	16	24	40
54	1	3	0	27	54	0	81
64	0	0	3	0	0	48	48
72	1	2	1	36	48	18	102
81	0	4	0	0	108	0	108
96	1	1	2	48	32	48	128
108	0	3	1	0	108	27	135
128	1	0	3	64	0	96	160

An example of how the different types of junctions are used to feed an array of 24 elements is shown in Figure 33.

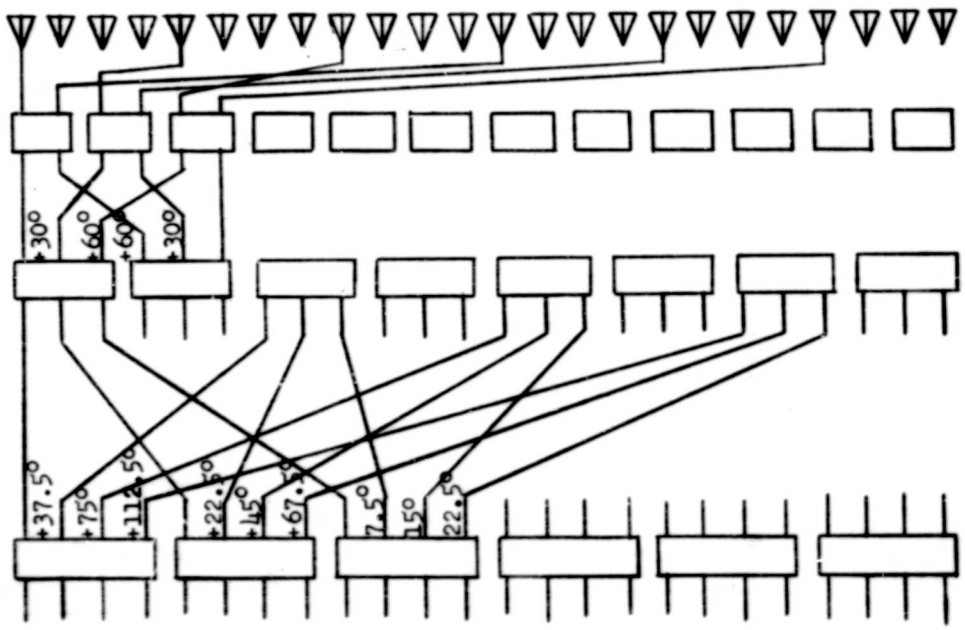

Figure 33. 24-Element Feed System Using Three Types of Junctions.

4.5 Conclusions

It has been shown that maximum space coverage is obtained by feeding an array of N elements with N feeds to provide N beams. Maximum efficiency is obtained by uniform illumination of all elements by all inputs; in fact, any illumination other than uniform, under the condition of maximum space coverage, is obtained only at the expense of transmission loss through the feed network.

Methods for synthesizing multiple-feed networks from building block junctions have been indicated. The simplest building block is the hybrid junction, and two other more complex junctions have been derived. At this point the number of beams is limited to $N = 2^l 3^m$.

Although the geometrical shape factor of the feed systems is somewhat complicated by overlapping lines, it is felt that this type of system represents an optimum case. Further study is indicated on modifications in this approach to allow reduction in space coverage, greater pattern control, and somewhat less efficiency.

V. CONCLUSIONS

Progress has been reported on research on scanning techniques for large, flat arrays. Effort to date has been concentrated on experimental investigation of smoothly variable phase shifters in open and enclosed transmission lines, theoretical studies on multiple-beam arrays and traveling-wave arrays, and analysis of circularly polarized phase shifters.

Significant new results have been achieved in the areas of multiple beams from linear arrays and wide-angle matching of traveling-wave arrays. In addition, an unusually compact and versatile phase shift mechanism has been conceived and is under development.

At this point it is worthwhile to consider the over-all goals of this contract as set forth in the statement of work and the specific goals defined in Status Report No. 1, 1 July 1959. Upon inspection of these, it is found that, in addition to the completion of programs in progress, such as the rotary phase shifter, increased emphasis is required on the array design as a whole. The following program is outlined for future effort:

1) Continue experimental phase shift investigation.
2) Consider system application of phase shift techniques, such as cascading units, providing two outputs with opposite phase, and the like.
3) Investigate scanning array problems such as low-elevation scanning and two-dimensional distribution and phasing.
4) Continue multiple-feed study with the goal of distribution control with reasonable efficiency.
5) Based on results from the first four items, design communication arrays for use at frequencies of approximately 80 mc, 240 mc, and 800 mc.

When the sample designs have been made, an appropriate experimental model can be decided upon through discussion by AGA and AFCRC personnel.

APPENDIX A - SIX-PORT JUNCTION FOR MULTIPLE-FEED ARRAYS

No systematic design procedure was used in deriving the designs for the six-port and eight-port junctions. In this appendix some of the considerations involved in finding networks to match the desired scattering matrices are given. The scattering matrices for six- and eight-port junctions are as follows:

$$1/\sqrt{3}\begin{pmatrix} 0 & 0 & 0 & e^{j\frac{2\pi}{3}} & 1 & e^{-j\frac{2\pi}{3}} \\ 0 & 0 & 0 & 1 & 1 & 1 \\ 0 & 0 & 0 & e^{-j\frac{2\pi}{3}} & 1 & e^{j\frac{2\pi}{3}} \\ e^{j\frac{2\pi}{3}} & 1 & e^{-j\frac{2\pi}{3}} & 0 & 0 & 0 \\ 1 & 1 & 1 & 0 & 0 & 0 \\ e^{-j\frac{2\pi}{3}} & 1 & e^{j\frac{2\pi}{3}} & 0 & 0 & 0 \end{pmatrix}$$

$$1/2\begin{pmatrix} 0 & 0 & 0 & 0 & e^{j\frac{3\pi}{2}} & e^{j\frac{3\pi}{4}} & e^{-j\frac{3\pi}{4}} & e^{-j\frac{3\pi}{2}} \\ 0 & 0 & 0 & 0 & e^{j\frac{3\pi}{4}} & e^{j\frac{\pi}{4}} & e^{-j\frac{\pi}{4}} & e^{-j\frac{3\pi}{4}} \\ 0 & 0 & 0 & 0 & e^{-j\frac{3\pi}{4}} & e^{-j\frac{\pi}{4}} & e^{j\frac{\pi}{4}} & e^{j\frac{3\pi}{4}} \\ 0 & 0 & 0 & 0 & e^{-j\frac{3\pi}{2}} & e^{-j\frac{3\pi}{4}} & e^{j\frac{3\pi}{4}} & e^{j\frac{3\pi}{2}} \\ e^{j\frac{3\pi}{2}} & e^{j\frac{3\pi}{4}} & e^{-j\frac{3\pi}{4}} & e^{-j\frac{3\pi}{2}} & 0 & 0 & 0 & 0 \\ e^{j\frac{3\pi}{4}} & e^{j\frac{\pi}{4}} & e^{-j\frac{\pi}{4}} & e^{-j\frac{3\pi}{4}} & 0 & 0 & 0 & 0 \\ e^{-j\frac{3\pi}{4}} & e^{-j\frac{\pi}{4}} & e^{j\frac{\pi}{4}} & e^{j\frac{3\pi}{4}} & 0 & 0 & 0 & 0 \\ e^{-j\frac{3\pi}{2}} & e^{-j\frac{3\pi}{4}} & e^{j\frac{3\pi}{4}} & e^{j\frac{3\pi}{2}} & 0 & 0 & 0 & 0 \end{pmatrix}$$

The form of the scattering matrices suggests the use of parallel-coupled transmission lines[15]. If a set of parallel coupled transmission lines is used, with all inputs on one side and outputs on the other, the requirements for match and isolation are automatically met. The simplest procedure is to find configurations that divide the input energy equally among all outputs, and then to try to arrive at proper phase outputs through trial and error.

Before the possible configurations are analyzed, it is worthwhile to consider the various types of coupling mechanisms. Shown in Figure 34 are

Configuration	Normal Modes	Propagation Constants
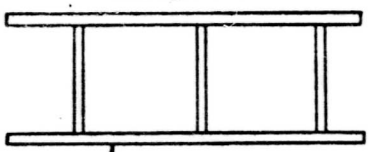 Center conductor of TEM line	+1 , +1	$\beta = \beta_o + C$
	+1 , -1	$\beta = \beta_o - C$
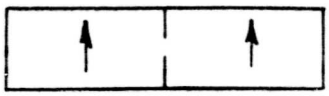 End View of Coupled Guides	+1 , +1	$\beta = \beta_o + 2C$
	+1 , -1	$\beta = \beta_o$
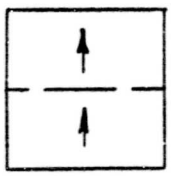 End View of Coupled Guides	+1 , +1	$\beta = \beta_o$
	+1 , -1	$\beta = \beta_o + 2C$

FIGURE 34. VARIOUS TYPES OF COUPLING MECHANISMS

branch coupling, waveguide narrow-wall and broad-wall coupling. The normal modes are the same for all cases -- even and odd, but the coupling characteristics yield different propagation constants for the modes. The following coupling relationships are deduced:

$$\begin{aligned} \beta E_1 &= \beta_o E_1 + cE_2 && \text{for branch coupling} \\ \beta E_1 &= \beta_o E_1 + c(E_2 + E_1) && \text{for side-wall coupling} \\ \beta E_1 &= \beta_o E_1 + c(E_2 - E_1) && \text{for broad-wall coupling} \end{aligned}$$

If the network of Figure 35 is assumed, in which the input line is coupled to N-1 other lines, it is of interest to determine the limitation on N for equal energy division among all outputs. The propagation constant matrix is found to be, for broad-wall coupling,

$$\begin{bmatrix} \beta_o-\beta + (N-1)c & -c & -c & -c & \cdots \\ -c & \beta_o-\beta + c & 0 & 0 & \\ -c & 0 & \beta_o-\beta + c & 0 & \\ -c & 0 & 0 & \beta_o-\beta + c & \\ \cdots & & & & \end{bmatrix}$$

Since, for input at E_1, all other outputs are identical in amplitude and phase, it is possible to reduce the matrix to a two-by-two array,

$$\begin{bmatrix} \beta_o-\beta + (N-1)c & -(N-1)c \\ -c & \beta_o-\beta + c \end{bmatrix}$$

Solution of the secular equation formed by setting the determinant of the propagation matrix equal to zero,

$$(\beta_o-\beta)^2 + (\beta_o-\beta)Nc = 0,$$

yields the two normal mode constants for the simplified system,

$$\begin{aligned} \beta_o-\beta &= 0 \\ \beta_o-\beta + Nc &= 0. \end{aligned}$$

The normal modes are found to be

$$\begin{aligned} E_1 &= E_2 \text{ for } \beta = \beta_o \\ E_1 &= -(N-1)E_2 \text{ for } \beta = \beta_o - Nc. \end{aligned}$$

For an initial input amplitude $E_1 = N$, E_2 through $E_N = 0$, it is found that the outputs are

$$E_1 = (N-1) + e^{-jNcx}$$

$$E_2 \cdots E_N = e^{-jNcx} - 1$$

where x is the length of the coupling region. Since the total input power is N^2, the output energy in each arm must be N, and the output amplitudes are $\sqrt{N}$.

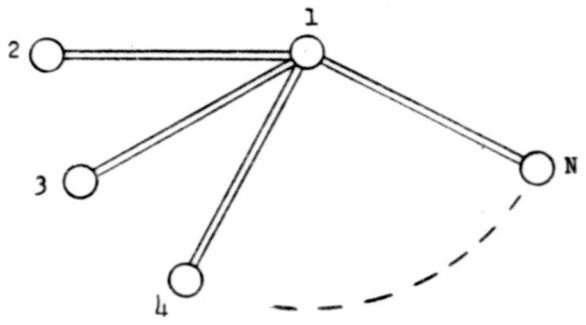

End View of Coupled Transmission Lines

Figure 35. Case for N-1 Lines Coupled to Input Line.

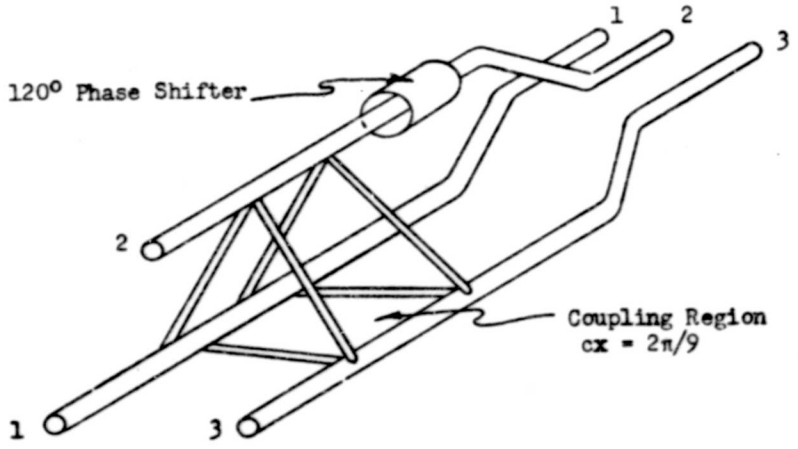

Figure 36. Three-Line Junction for Multiple-Feed Arrays.

It is easily seen that the output amplitude is, with the exception of phase, $2 \sin \frac{Ncx}{2}$. Thus, the condition for achieving equal power division is

$$2 \sin \frac{Ncx}{2} \leq \sqrt{N}$$

For $N = 2$ $cx = \pi/4$
$N = 3$ $cx = 2\pi/9$
$N = 4$ $cx = \lambda/4$

For $N > 4$, the condition cannot be satisfied; it is, therefore, seen that the arrangement of Figure 35 is limited to four lines.

If three lines are all coupled by an amount $cx = 2\pi/9$, as shown in Figure 36, the relative phases of the outputs are

	1	2	3
Input at 1	0°	+120°	+120°
Input at 2	+120°	0°	+120°
Input at 3	+120°	+120°	0

If a phase shift of +120° is introduced into the output of line 2, the relative phases become

	1	2	3
Input at 1	0°	-120°	-240°
Input at 2	0°	0°	0°
Input at 3	-240°	-120°	0°

and this is desired phase relationship.

It is easily shown that the other two types of coupling mechanisms can be used to realize the same type of network, except that the required added phase shift may be positive or negative, depending on the type of coupling.

APPENDIX B. FOUR-INPUT FOUR-OUTPUT JUNCTION FOR MULTIPLE-FEED ARRAYS

The two coupling configurations shown in Figure 37 can be shown to give equal output amplitudes for coupling regions having $cx = \pi/4$. The phase relationship of the outputs for input at line 1 is

	1	2	3	4
Case A	0°	-90°	-90°	-180°
Case B	0°	-180°	-180°	-180°

It is impossible to achieve the required phase characteristics using only one coupling configuration. The network of Figure 38 combines both types and gives the following phases:

	1	2	3	4
Input at 1	0°	-90°	-90°	-180°
Input at 2	-180°	0°	-180°	-180°
Input at 3	-180°	-180°	0°	-180°
Input at 4	-180°	-90°	-90°	0°

If the outputs are rearranged as shown and the indicated phase shifts are added, the resultant behavior provides multiple-feed capability.

	1	2	4	3
Added phase shift	0°	-45°	-90°	+45°
Input at 1	0°	-135°	-270°	-405°
Input at 2	0°	+135°	+270°	+405°
Input at 3	0°	-45°	-90°	-135°
Input at 4	0°	+45°	+90°	+135°

It will be noted that a lagging phase shift has been assumed in this case. The reason is that the two coupling arrangements of Figure 37 must be combined so that they operate essentially independently. That is, for an input to line 1, lines 2 and 3 are uncoupled, and for an input to line 2, lines 1, 3 and 4 are uncoupled. This is achieved only for difference coupling, for which the coupling term is of the form $c(E_2 - E_1)$, so that when the amplitudes are the same the coupling is zero.

Difference coupling is characteristic of broad-wall connection between waveguides. It can be obtained with branch networks only at the expense of an awkward increase in complexity. Some of the possible waveguide cross sections for the three-line junction and the two cross sections for a four-line junction are shown in Figure 39.

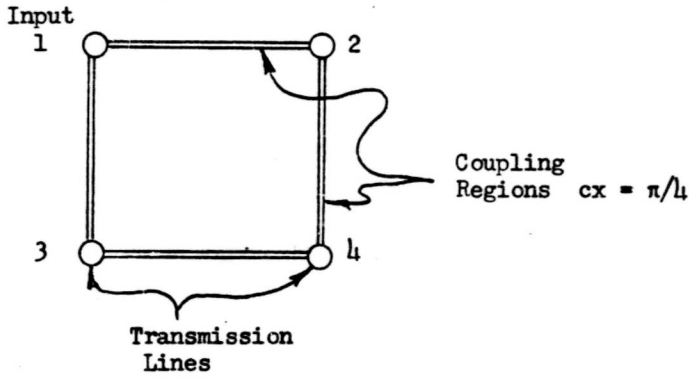

CASE A.

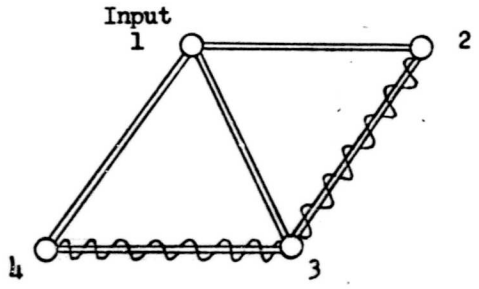

CASE B.

FIGURE 37. COUPLING CONFIGURATIONS FOR EQUAL POWER DIVISION WITH FOUR LINES.

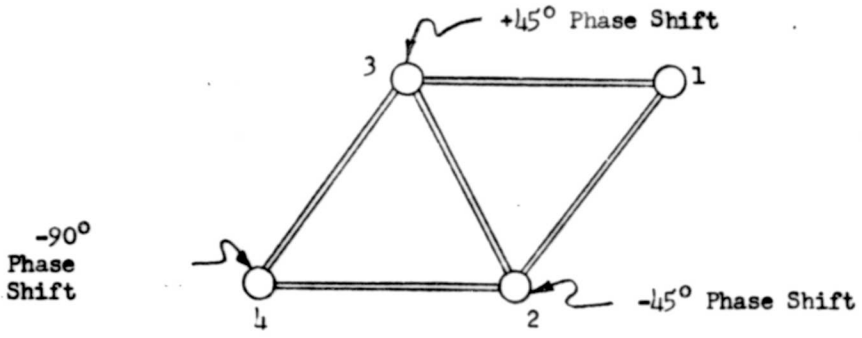

Figure 38. Four-Line Network with Multiple-Feed Capability.

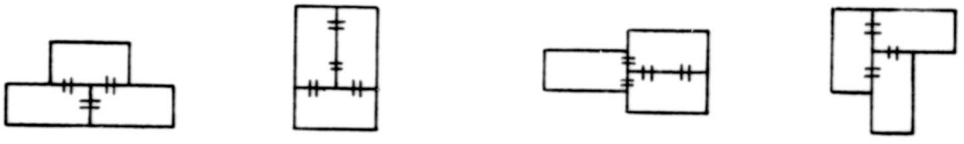

(a) Waveguide Orientations for Three-Line Couplers.

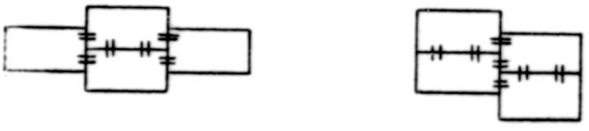

(b) Orientations for Four-Line Coupler.

Figure 39. Allowable Waveguide Arrangements for Couplers of Three and Four Lines

VI. REFERENCES

1. Georg Goubau, "Designing Surface Transmission Lines," Electronics, Vol. 27, No. 4, pp. 180-184; April 1954.

2. Sichak and Milazzo, "Antennas for Circular Polarization," Proc. IRE; Vol. No. 35, August 1947.

3. A. Gardner Fox, "An Adjustable Waveguide Phase Changer," Proc. IRE; Vol. No. 35, December, 1947.

4. B. M. Schiffman, "A New Class of Broad-Band Microwave 90-Degree Phase Shifter," Trans. IRE, Vol. MTT-6, No. 2, April 1958.

5. S. R. Seshadri and K. Lizuka, "A Dipole Antenna Coupled Electromagnetically to a Two-Wire Transmission Line," Prepared by Harvard University for AFCRC, Contract AF19(604)-786, dated October 31, 1958.

6. C. J. Sletten and G. R. Forbes, "A New Antenna Radiator for VHF-UHF Communications," Prepared by AFCRC TR-57-114; June, 1957.

7. Sletten, Holt, Blacksmith, Forbes, Shodin and Henkel, "A New Single Antenna Interferrometer System Using Proximity Coupled Radiators," Prepared by AFCRC TR58-115, March, 1958.

8. A. A. Laport, "Open-Wire Radio-Frequency Transmission Lines," Proc. IRE, Vol. 31, No. 6, pp. 271; June, 1943.

9. D. M. Bowie and G. G. Chadwick, "A New Eagle Type Scanner," AFCRC Electronic Scanning Symposium; April 29, 30 - May 1, 1958.

10. W. E. Kock, "Metallic Delay Lenses," BSTJ, Vol. 27, No. 1, pp. 58-82; January 1948.

11. R. K. Moore, "The Effects of Reflections From Randomly Spaced Discontinuities in Transmission Line," Trans. IRE, Vol. MTT-5, No. 2, pp. 121-126; April 1957.

12. J. A. Mullen and W. L. Pritchard, "The Statistical Prediction of Voltage Standing-Wave Ratio," Trans. IRE, Vol. MTT-5, No. 2, pp. 127-130; April, 1957.

13. M. Carroll, W. Kahn, E. Shubel, "Multidirectional Beam Scanning Antenna Array - First Interim Report," prepared for RADC by W. L. Maxson Corp., Contract No. AF30(603)-1920; July, 1958 - April, 1959.

14. L. Joseph and W. K. Saunders, "A Theorem on Lossy Nonreciprocal N-Port Junctions," Proc. IRE, Vol. 47, No. 1, pp. 102; January, 1959.

15. J. P. Shelton, Jr., "Multiple-Line Directional Couplers," IRE National Conv. Record, Vol. 7, Part 1; 1957.

AD

235 571